



저작자표시-비영리-변경금지 2.0 대한민국

이용자는 아래의 조건을 따르는 경우에 한하여 자유롭게

- 이 저작물을 복제, 배포, 전송, 전시, 공연 및 방송할 수 있습니다.

다음과 같은 조건을 따라야 합니다:



저작자표시. 귀하는 원저작자를 표시하여야 합니다.



비영리. 귀하는 이 저작물을 영리 목적으로 이용할 수 없습니다.



변경금지. 귀하는 이 저작물을 개작, 변형 또는 가공할 수 없습니다.

- 귀하는, 이 저작물의 재이용이나 배포의 경우, 이 저작물에 적용된 이용허락조건을 명확하게 나타내어야 합니다.
- 저작권자로부터 별도의 허가를 받으면 이러한 조건들은 적용되지 않습니다.

저작권법에 따른 이용자의 권리는 위의 내용에 의하여 영향을 받지 않습니다.

이것은 [이용허락규약\(Legal Code\)](#)을 이해하기 쉽게 요약한 것입니다.

[Disclaimer](#)

공학박사 학위논문

Hydroxyapatite coating using sol-gel
method to increase osseointegration of
zirconia as a dental implant

치과용 임플란트로서의 지르코니아의 골적합성을 증가시키기
위한 졸 젤 법을 활용한 하이드록시아파타이트 코팅

2021년 8월

서울대학교 대학원

재료공학부

김진영

Hydroxyapatite coating using sol-gel
method to increase osseointegration of
zirconia as a dental implant

치과용 임플란트로서의 지르코니아의 골적합성을 증가시키기
위한 졸 젤 법을 활용한 하이드록시아파타이트 코팅

지도교수 김 현 이

이 논문을 공학박사 학위논문으로 제출함

2021년 8월

서울대학교 대학원

재료공학부

김 진 영

김 진 영의 박사 학위논문을 인준함

2021년 6월

Chair 안 철 희

Vice Chair 김 현 이

Examiner 선 정 윤

Examiner 한 철 민

Examiner 정 현 도

Abstract

Hydroxyapatite coating using sol-gel method to increase osseointegration of zirconia as a dental implant

Jinyoung Kim

Department of Materials Science and Engineering

Seoul National University

Dental implants for replacing teeth lost for various reasons are widely used hard tissue implants. The most widely used material for dental implants is titanium (Ti), which has excellent strength and biocompatibility. However, titanium can have an aesthetic rejection because of its unique shiny surface, and non-specific immune reactions in the metal and corrosion by biomaterials such as saliva are problematic. Meanwhile, zirconia is attracting attention as a new dental implant material in that it is free from corrosion and immune reactions, as well as excellent mechanical properties and aesthetic effects. However, zirconia has a disadvantage in that it has relatively low bone compatibility. Hydroxyapatite is a biocompatible ceramic that exists in a large number of human bones as a representative

component of human bone. Due to its unique excellent biocompatibility, it is used as a material for coating the surface of numerous biomaterials. There have been many studies related to hydroxyapatite (HA) coating for improving the biocompatibility of zirconia, but there is a problem with a thick thickness and deterioration of stability due to by-product formation in high-temperature sintering.

In this study, to increase the biocompatibility of zirconia, we intend to coat hydroxyapatite using the sol-gel method. The sol-gel method is used to further improve biocompatibility by changing the nano and micro structures of the coating layer, and to form a thin and stable hydroxyapatite coating layer without by-products by controlling the sintering temperature.

First, in order to change the surface structure of the hydroxyapatite coating layer, the sintering temperature and the aging time of the hydroxyapatite sol were adjusted, and the surface structure was observed through scanning electron microscope (SEM) observation. It was found to have an effect on the microstructure. In addition, through transmission electron microscopy (TEM) observation, the change in the particle size in the hydroxyapatite sol according to the aging time was confirmed, and this change was found to be the cause of the change in the microstructure of the coating layer. When the thickness was measured through a focused ion beam (FIB), it was confirmed that the coating layer had a size of about 150 nm, and the portion having a microstructure had a size of about 800 nm. In addition, through non-contact 3D surface analysis, it was confirmed that when Ra has a microstructure, it is about 350 nm, which is higher than about 100 nm when there is no microstructure. In addition, when the sintering temperature was 800 °C through X-ray diffraction analyzer (XRD) and X-ray photoelectron spectroscopy (XPS), there was no crystal phase other than HA and

zirconia. It was confirmed that was generated. The contact strength between the coating layer and the zirconia was conducted by a tensile test through Instron, and had a value of about 40 MPa or more, which was suitable for dental implant applications.

Cell experiments were conducted through osteoblasts by controlling the formation of microstructures under conditions of 800 °C, and it was confirmed that the *in vitro* cell characteristics increased when the microstructure was formed. Based on this, as a result of conducting *in vivo* animal experiments on zirconia and zirconia coated with hydroxyapatite along with titanium as a comparative group, it was proved that the bone compatibility of zirconia was dramatically improved by hydroxyapatite coating, which is similar to that of conventional titanium implants.

Through this study, it was possible to achieve an increase in the bone compatibility of zirconia through hydroxyapatite. In addition, by controlling the aging time and sintering time of the hydroxyapatite sol, the nano and microstructure of the coating layer could be controlled. In particular, by controlling the sintering time, the formation of calcium zirconate, a by-product of zirconia and hydroxyapatite, could be suppressed. It was proved through *in vitro* cell experiments and *in vivo* animal experiments that the sol gel-based HA-coated zirconia produced based on this has great potential for use as a dental implant material.

Keyword : Dental implant, Zirconia, Hydroxyapatite, Surface modification, Sol–gel, Osseointegration

Student Number : 2016–20779

Table of Contents

Abstract.....	i
List of Tables.....	vii
List of Figures.....	viii
Chapter 1. Introduction.....	1
1.1. Biomaterials for dental implant.....	2
1.2. Hydroxyapatite coating for enhancing osseointegration.....	4
1.3. Issue of hydroxyapatite coating on zirconia Introduction.....	6
1.3.1. surface modification of hydroxyapatite coating layer.....	8
1.3.2. limitation of hydroxyapatite coating on zirconia	13
1.4. Purpose of this study	15
Chapter 2. Materials and methods	19
2.1. Materials for HA-coated zirconia	20
2.1.1. Preparation of the zirconia substrates.....	20
2.1.2. Ha sol synthesis	20
2.2. HA-coated zirconia preparation.....	21
2.3. Characterization of HA-coated zirconia.....	22
2.4. <i>In-vitro</i> osseointegration of the HA-coated zirconia	23
2.5. <i>In-vivo</i> osseointegration of the HA-coated zirconia	24

2.6. Statistical analysis.....	26
Chapter 3. Results and discussion.....	30
3.1. Control the surface morphology of the HA layer	31
3.1.1. Sintering temperature	31
3.1.2. HA sol aging time	33
3.2. Control the reaction of HA and zirconia by adjusting sintering temperature	37
3.2.1. Characteristics of HA coated zirconia with various sintering temperature	37
3.2.2. Coating stability of HA coated zirconia	40
3.3. Comparison of HA-coated zirconia with and without micro roughness	43
3.4. <i>In-vitro</i> osseointegration of the HA-coated zirconia	46
3.4.1. Osteoconductivity of roughness difference.....	46
3.4.2. Osteoconductivity of HA-coated zirconia.....	47
3.5. <i>In-vivo</i> osseointegration of the HA-coated zirconia	48
Chapter 4. Conclusions	68
4.1. Conclusions.....	69

Reference.....	73
Abstract in Korean	89

List of tables

Table.2.1. Experimental conditions.

List of figures

Figure.1.1. schematic of the interactions between bone and the implant surface at different topographical scales.

Figure.1.2. Schematic images of the HA coated zirconia implant of this study.

Figure 2.1. Schematic representation of experimental procedure.

Figure.2.2. schematic images of adhesion strength test.

Figure.3.1. surface morphology of HA coated zirconia which sintered at various temperature; (a) bare, (b) 400 °C, (c) 600 °C, (d) 800 °C, (e) 1000 °C scale bar: 5 μm (large), 1 μm (inset).

Figure.3.2. surface morphology of HA coated zirconia with various HA sol aging time, (a) 3h, (b) 1d, (c) 3d, (d) 5d. Scale bar: 50 μm (large), 2 μm (inset).

Figure.3.3. TEM images of dried HA sol with various aging time, (a) 3h, (b) 1d, (c) 3d, (d) 5d. Scale bar: 100 nm(large), 10 nm(inset).

Figure.3.4. (a) TEM image and (b) FFT image of dried 1d aging HA sol.

Figure 3.5. Viscosity of HA sol with various aging time and Ethanol (solvent).

Figure.3.6. XRD patterns of the HA-coated zirconia substrates with various sintering temperatures; 2θ range of 20 – 60 degree (a),

31–37 degree (b).

Figure.3.7. XPS data of HA-coated zirconia substrates with 800 °C (a) and 1000 °C (b) sintering temperature and Oxygen binding energy of 800 °C (c) and 1000 °C (d).

Figure 3.8. SEM images of the failure surfaces of the bare and HA-coated zirconia after the adhesion test: (a) bare zirconia, (b) HA600, (c) HA800, and (d) HA1000. The black and yellow dotted lines indicate the areas where the stud adheres to and epoxy remains, respectively. Scale bars: 500 nm.

Figure.3.9. Adhesion strength of the HA-coated zirconia substrates with various sintering temperatures.

Figure.3.10. Thickness of HA coated zirconia using 1d aging HA sol (a) and 3d aging HA sol (b)

Figure.3.11. Surface roughness of HA coated zirconia using 1d aging HA sol (a) and 3d aging HA sol (b). Rq and Ra value of HA coated zirconia (c).

Figure.3.12. XRD analysis of HA coated zirconia using 1d aging HA sol and 3d aging HA sol.

Figure.3.13. SEM images of cells attached on the HA coated zirconia using 1d aging HA sol (a) and 3d aging HA sol (b).

Figure.3.14. Confocal laser scanning microscope image of the cells attached on the HA coated zirconia using 1d aging HA sol (a) and

3d aging HA sol (b) and cell coverage area (c). Scale bars: confocal image (20 μm).

Figure.3.15. Confocal laser scanning microscope image of cells attached on the (a) Ti, (b) bare, and (c) HA-coated zirconia surfaces with cell coverage area (d). Scale bars: confocal image (20 μm).

Figure 3.16. Degree of proliferation of the MC3T3-E1 cells on the Ti, bare, and HA-coated zirconia substrates after 3 and 5 days of seeding.

Figure 3.17. Representative histological cross-sectional image of the stained slices after 6 weeks of implantation: (a, d) Ti, (b, e) bare, and (c, f) HA-coated zirconia. O and N indicate the old and new bone areas, respectively. Scale bars: (a-c) low-magnification image (2 mm) and (d-f) high magnification images (200 μm).

Figure 3.18. (a) Bone-to-implant contact and (b) new bone area ratios of Ti, bare-, and HA-coated zirconia.

Chapter 1. Introduction
(Theoretical Review)

1.1. Biomaterials for dental implant

As the life expectancy of people increases with advances in infrastructure and medical technology, the importance of tissue engineering to develop implants to replace various tissues was increasing [1, 2]. Among them, dental implants were one of the most widely used and successfully established implants in various hard tissue engineering. Dental implants were largely composed of a screw that connects to the gums, a crown that replaces the teeth, and an abutment that connects those, and recently, a screw and abutment were combined to form a single part. These parts had different capabilities depending on their respective roles. The externally visible crown had an aesthetic role, the abutment that was relatively easy to expose to bacteria had antibacterial properties, and the screw connecting the gum bone and dental implant had high strength. In addition, osseocompatibility was required for the screw to make a firm contact with the gingival bone. In particular, the screw was an important component that most critically affect the success of dental implant placement. If the screw was damaged after implantation due to weak strength, or if it did not contact the gingival bone due to poor bone compatibility, it may cause implantation failure.

For this reason, it could be seen that titanium was the most widely used material for screws of dental implants as it was a material with

excellent bone compatibility and strength [3, 4]. Titanium was a widely known metal with excellent bioproperties, especially bone compatibility, and was used not only for dental implants but also for implants in the orthopedic field [5]. However, in various studies, problems that may arise when titanium was used for dental implants were being discussed. Non-specific immune reactions or autoimmunity caused by metal, galvanic side effects occurring in contact with saliva or fluoride, and, although very rare, allergic reactions to titanium had been reported. In addition to this, the lustrous grayish color characteristic of the metal sometimes causes antipathy in the aesthetic part [6-8].

Ceramic implants had been studied to overcome these problems, but there was always a risk of fracture due to the brittleness of ceramics, making it difficult to find alternatives [9]. However, recently, yttria-reinforced zirconia had been used in various orthopedic fields, and it had been demonstrated that there was no risk of fracture with sufficient strength and flexural strength [10-16]. In addition, it could be free from problems such as non-specific immune response and galvanic side effect because of its significantly lower ion emission and bioinert properties compared to titanium, a metal implant [17, 18]. In addition, zirconia had the advantage of not giving an aesthetic objection as it had almost the same color as a tooth to the extent that

it was also used as a crown. Despite the various advantages suitable for use in dental implants, zirconia had a fatal disadvantage that it does not have excellent bone compatibility, and various studies were being conducted to overcome it [14, 19, 20].

Hydroxyapatite was one of the substances that make up bones in the human body and is one of the most abundant substances in the living body. As such, it had excellent bone compatibility and was used as a material for bone substitutes in various ways [21-23]. However, in the case of hydroxyapatite, it was difficult to use as a scaffold that should serve as a support by replacing damaged areas because it had a weak strength and was very easily cracked, which was characteristic of ceramics [24]. Instead, it was often used as a coating material for various biomaterials in order to preserve the unique biocompatibility.

1.2. Hydroxyapatite coating for enhancing osseointegration

As a method of improving bone compatibility, the most representative and widely used method was to control the surface of the implant. Typically, there was a method of increasing the surface roughness or a method of coating the surface with a material having excellent bone compatibility. Among them, hydroxyapatite was used as a coating material for various materials due to its excellent bone

compatibility [25]. It was also used as a coating material to further increase the bone compatibility of titanium, which was known to have good biological properties, and was also used as a coating material to increase the bone compatibility of other alumina, ceramics, and even polymers [26-28]. There were various methods for coating HA. It could be coated on the surface in various ways by depositing it on the surface through SBF (Stimulated Body Fluid), forming a surface layer through slurry, and using HA sol generated through the sol-gel method [29, 30]. In particular, if the sol-gel method was used, the coating material was prepared in a liquid form, so it was possible to use all methods from the simplest dip coating to spin coating and spray coating. In addition, there were several methods for making the HA coating layer through physical vapor deposition (PVD) or other methods. According to H.W.Kim et al, after coating the titanium surface with Hydroxyapatite through the sol-gel method, cell characteristics through osteoblasts were evaluated, and a marked increase was observed [31]. H. Deplaine et al. attempted to coat HA to increase the osteocompatibility of the polymer PLA scaffold [32]. Unlike metals and ceramics, in the case of polymers, most coating methods including sintering could not be used because the method using heat could adversely affect the substrate, and precipitation through SBF was used. Through this, it was possible to create a

unique thorn-shaped HA coating layer, and an increase in bone compatibility was confirmed through animal experiments. As such, HA was a material that can be considered at least once to improve the bone compatibility of scaffolds for bone replacement.

1.3. Issue of hydroxyapatite coating on zirconia

As such, a method of increasing bone compatibility by coating HA through various methods was also used in dental zirconia implants. Coating was done through SBF, and various methods such as coating through slurry and coating through sol-gel method were applied [33]. In addition, various coating methods such as electrophoretic deposition, coating used by sputter, plasma spraying, pulsed laser deposition coating, and HIP were used, and it was confirmed that bone compatibility was increased through coating. All methods had their own advantages and disadvantages [34-36]. Representatively, according to Y.Cho et al., it was possible to simply coat HA on zirconia through the aerosol deposition method, and through this, it was possible to confirm the increase in bone compatibility [8]. However, the thickness at this time was very large, about 10 μm , so there was a disadvantage in that the coating layer was unstable. In addition, Hasan et al. were able to achieve a ZrO_2/Hap composite coating using the plasma spraying technique and increase the cell

properties [37]. However, this method had problems such as residual stress and non-uniformity of the coating layer in a complicated shape (ex. screw shape). In order to apply it to Zirconia dental implant, the bonding strength of the coating layer must be good, it must be uniformly coated even in a complex shape, and the condition was that it does not adversely affect both the coating layer and the substrate. However, although various types of HA coating methods were used for zirconia implants, there were problems in the stability of the coating layer, application to complex shapes, and economic efficiency. Among them, the coating method through the sol-gel method could form the thinnest coating layer, which helps the stability of the HA layer, could be coated simply, and was in the form of a solution, so various coating methods (ex. spray coating, spin coating, dip coating) could be used, so it was considered an effective method that could be used for complex shapes [38, 39]. However, there was a problem that the sol-gel method must undergo through the process of sintering after coating. In this study, among the various problems that might occur when using the sol-gel method in this study, the first thing to note was that there was no study on the surface structure after coating, and the by-product problem by reaction of the material when sintering at high temperature to obtain the crystallinity of zirconia and HA.

1.3.1. surface modification of hydroxyapatite coating layer

Various papers had shown that surface structure influences cell properties [40–43]. It was known that the following processes occur when cells react and grow on the surface of the scaffold. First, cells check whether this surface is a good surface to contact, and then make contact. After that, they proliferate through signaling between the surface and cells and between cells, and through the process of differentiation, growth into a tissue was achieved. The most important process in this process was also the contact with the surface, because if the surface and cells of the implant do not contact the surface due to poor cell characteristics, all subsequent processes could not be completed. It was known that the cell fitness of the implant surface was affected by the following topography, wettability, charge, pore size, and bioactivity by drugs [44]. In particular, topography, including roughness, greatly affect the cell suitability of the surface, and both micro and nano roughness appear to affect cell properties. Regarding the reason, Rolando et al. said that micro roughness made the surface micro-sized protrusions directly interact with osteoblasts or mesenchymal stem cells, which were the main agents for bone regeneration [45]. In addition, roughness at the nano level makes it easier for proteins to adsorb between them, and

receptors on the cell membrane, including integrins, recognize this and claim that it could help cell adhesion.

Therefore, improvement of cellular properties was induced by controlling the surface structure of various materials, especially micro and nano level roughness. In particular, the aforementioned titanium was already known to have excellent biological properties, but in order to further increase the roughness, various surface treatment methods were used to increase the roughness. Typically, micro-level roughness was controlled on the surface by sandblasted, larger-grit and acid etched (SLA) method, anodizing, and micro arc oxidation (MAO), and recently, nano level roughness was controlled through target ion induced plasma sputtering (TIPS) method [5, 46]. It was confirmed that the cell properties were increased through these various roughness control methods.

Similarly, hydroxyapatite, which had excellent cell properties, tried to increase cell properties through various surface treatments. The method of adding other elements such as fluorine or silicon, the method of attaching various functional groups, and the method of supporting proteins or drugs with good cell characteristics were commonly used [47]. However, only a few studies tried to directly control the topography, and many studies focused on the coating itself rather than the topography. Methods for controlling topography

include polymer demixing, injection moulding, microprinting, photo and electron beam lithography with wet chemical etching. Among them, photo and electron beam lithography with wet chemical etching method was the most widely used recently. Briefly, first, a photoresist material was coated on a substrate, a circuit of a desired shape was manufactured, and a positive or negative pattern could be created by irradiating light including UV on it. After that, after removing the remaining resist through a chemical etching method, HA was coated through various methods to create micro and nanostructures. Through this related study, an HA coating layer was created on various biocompatible materials, and it was confirmed that the biocompatibility was increased through this method. However, these methods have disadvantages such as high risk of failure, cumbersome, and expensive as they go through several processes.

Then, it was necessary to find conditions for controlling the surface structure of HA-coated zirconia using the sol-gel method. There were various conditions that could be controlled in the course of the experiment, but the essential among them were the preparation of HA sol, dip coating conditions, and sintering. Among them, dip coating conditions affect the thickness, so it was not suitable for comparison of surface structures. Therefore, it was considered the best situation if the surface structure could be controlled by changing

the HA sol manufacturing conditions and sintering conditions [48–50]. It was believed that the influence on the surface structure was the size of the HA grains in the HA coating layer and the particle size of the HA sol itself. In various papers, it could be seen that the sintering temperature has a very large effect on the grain size of the ceramic [51]. HA was no exception. As shown in the following equation (1), it was well known that the particle size of HA change with the sintering temperature. At this time, D represents the average grain size, Q represents the activation energy, and the activation energy value of HA was known to be approximately 54 ~ 59 kcal/mol. Therefore, it could be confirmed that the grain size increase as the sintering temperature increase, and accordingly, it could be expected that the surface structure become more and more flat. The following paper confirmed this, as confirmed by E. Saiz et al., the grain size was gradually increasing as the sintering temperature and time increase [52]. At this time, it could be seen that there was no significant difference in the sintering time, while the sintering temperature had a dramatic effect. In addition, it was also confirmed that the surface structure had a flat structure from the sintering temperature of about 1000 °C.

$$D = A \exp(Q/RT) \quad (1)$$

In addition, the sol-gel method was a method in which precursors

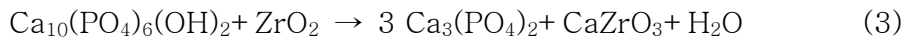
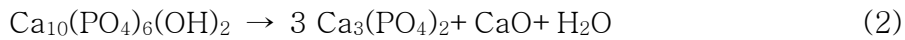
were mixed in a solvent at once and then particles were generated by diffusion and reaction through particle generation and growth of the particles. When the particles grow, the precursors adhere to the generated particles and grow, or the particles aggregate and merge with each other to grow [53-55]. The part to focus on here was the part where the particles aggregate and grow together, which could be called secondary growth. In that case, the size of the particles was different, and if it was a mixture of large and small particles, it was expected to have various surface structures when sintered after coating. Small particles were expected to have a coating structure of the overall surface, and large particles were expected to have a unique surface structure by making larger particles on the surface. Through this, it could be possible to create a surface structure with nano- and micro-roughness. The conditions of HA sol that could be controlled were the concentration of HA sol and the aging time, etc. Since various growth represented by secondary growth was required, it was reasonable to control the time required for growth, so set the aging time as a variable and conduct the experiment.

1.3.2. limitation of hydroxyapatite coating on zirconia

The method of coating hydroxyapatite on zirconia had been tried through several methods. However, as there were advantages in all methods, there were also disadvantages. The thickness of the coating layer was too thick, the HA coating layer could not be firmly combined with the zirconia substrate, or by-products were generated, which lowers the stability and bio-properties of the coating layer [56, 57]. In the end, when all these shortcomings were put together, the stability of the coating layer was good and there was no by-product. Specifically, looking at the following paper coated with SBF, the thickness of the coating layer could be controlled by controlling the time, but nevertheless, there was a disadvantage that the thickness of the coating layer itself was not stable because the thickness to see the effect of increasing bone compatibility was too thick. An attempt was made to reduce the thickness of the coating layer and increase the stability through the coating through the slurry, but a high-temperature sintering process was required to make HA, and the reaction between HA and zirconia occurred, resulting in the generation of calcium zirconate, a by-product.

During heat treatment, tricalcium phosphate is produced by the thermal decomposition of HA, as shown in Equation (2). This usually occurs above 1300 °C. However, when zirconia is present, the

reaction temperature could be lowered to 1000~1150 °C because the reaction occurs as Equation (3), and calcium zirconate is formed as a byproduct [58–60]. This phenomenon occurs at high temperatures because it provides sufficient mobility and time for the decomposition of HA to TCP and the reaction of CaO, a byproduct of decomposition, and zirconia [61]. Calcium zirconate, which is an unwanted by-product that is finally produced, not only degrades the mechanical properties, but also lowers the osteoconductivity of the coating layer [62, 63].



To solve this problem, the following papers used a method of introducing fluorinated hydroxyapatite as an intermediate layer, and through this, HA-coated zirconia at high temperature could be produced, but the inconvenience and stability caused by one additional process [64, 65]. The issue had to arise again. In addition, the PVD method was used to coat, but this method was able to make a coating layer stably without by-products, but there was a risk that the coating layer might be destroyed because the thickness was too thick with a size of about 100 μm. Taken together, it could be seen that making a stable HA coating layer through a different coating method was an important issue in the HA coating of zirconia.

1.4. Purpose of this study

In conclusion, the purpose of this study was to increase bone compatibility by forming a stable and thin HA coating layer on the zirconia dental implant. In addition to this, we want to adjust the surface structure so that the improvement of bone compatibility could be further increased. The method introduced for this purpose was HA coating through the sol-gel method. Sol-gel method referred to a method of making a sol in which small particles were dispersed in a solution and a gel formed by interconnecting these particles. This sol-gel method was the most representative to use when making powder that was used in various ways, but it could be made in the form of fibers using the sol state, and a coating layer with a film or pattern can be made, and the gel state was used. It was also possible to create porous structures such as monoliths. Among them, sol was easy to make a uniform coating layer on the substrate because of the characteristics that the particles were evenly dispersed. In addition, liquid sols allow almost any coating method that could be used in liquid state. Starting with dip coating, which was known to be the simplest, spin coating, spray coating, flow coating, blow coating, as well as electrodeposition and electrospinning using the electric properties of particles could be

used. Fortunately, HA could be made in sol form simply by mixing it evenly using a solution containing Ca source and a solution containing P source and then undergoing an aging process. And since almost any coating method could be used, it was used the dip coating method, which was the simplest and most economical way to create a thin coating.

In order to solve the above-mentioned issues, we try to control the coating process in various ways. To further increase the bone compatibility of the coating layer, we are trying to make nano and micro structures on the surface. To this end, by controlling the sintering temperature, the surface structure can have a nano structure by finding a temperature at which the surface structure does not become flat. In addition, to control the stability of the coating layer, a thin coating layer is created through dip coating, and the sintering temperature is adjusted to suppress the reaction between zirconia and HA to find a temperature with crystallinity through sintering without by-products.

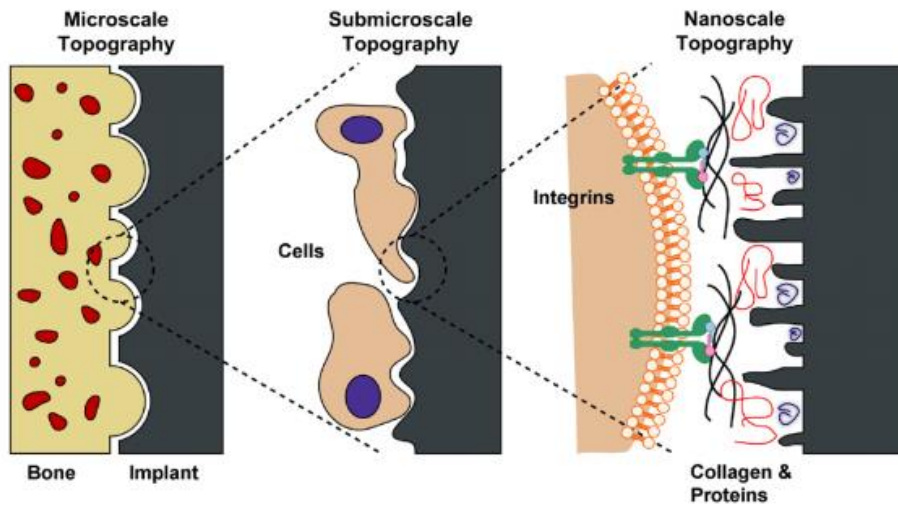


Figure.1.1. schematic of the interactions between bone and the implant surface at different topographical scales.

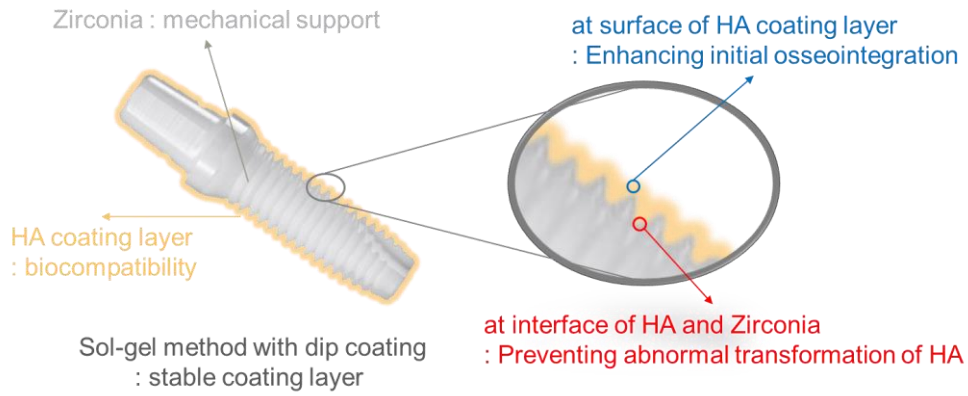


Figure.1.2. Schematic images of the HA coated zirconia implant of this study.

Chapter 2. Materials and methods

2.1. Materials for HA-coated zirconia

2.1.1. Preparation of the zirconia substrates

A plate-type zirconia substrate was used to optimize the coating conditions and evaluate the in vitro cellular behaviors. A zirconia block was produced by the following process: first, zirconia stabilized by 3 mol % of yttria powder (3Y-TZP, Tosoh Corporation, Japan) was compressed at 20 MPa, followed by the application of cold isostatic press at a pressure of 200–300 MPa and pre-sintering at 1100 °C; next, the block was cut into a plate shape with dimensions of 10 × 10 × 1 mm³; and the zirconia plate was then sintered at 1500 °C for 2 h at a heating rate of 5 °C/min. A screw-type zirconia substrate was also prepared by machining the zirconia block to screw shape with 2-mm diameter and 10-mm length to evaluate the osteoconductivity under the in vivo condition.

2.1.2. HA sol synthesis

First, 0.015 mol (2.494 g) of triethylphosphite (TEP, Sigma-Aldrich, USA) was added to a mixed solution of 23.92 ml ethanol (Daejung, Korea) and 1.08 ml deionized water. Second, 0.0251 mol (4.1102 g) of calcium nitrate tetrahydrate ($\text{Ca}(\text{NO}_3)_2 \cdot 4\text{H}_2\text{O}$, Sigma-Aldrich, USA) was dissolved in 25 ml ethanol. The

theoretical concentration of the final HA sol is 0.05M, assuming that all reactants have reacted. These solutions were mixed together at room temperature for 3 days and aged at 37 °C for 3 hours, 1 day, 3 days, 5 days with continuous stirring to make the HA sol. The upper part of figure.2.1. represented this process

2.2. HA-coated zirconia preparation

HA was coated on the zirconia plate and screw using the dip-coating technique. HA sol aged at 3 days was used to confirm the sintering temperature effect. The dip-coating rate was 0.25 mm/s and performed thrice. The sol was dried for 5 min in the oven at 37 °C between each dipping step. The HA-coated zirconia plate was oven-dried at 70 °C overnight and sintered at 400 °C, 600 °C, 800 °C, and 1000 °C for 1h at a heating rate of 5 °C/min after the coating was completed. Also, to confirm the HA aging time effect to surface morphology of HA coating layer, this process is repeated HA sol aged with various time. In this case, sintering temperature is fixed at 800 °C. Variables and fixed variables are summarized in Table 2.1. For the zirconia screw to using in-vivo study, excessive sol was trapped between the screw threads, which might cause an unwanted thick coating layer; thus, spinning was performed at 150 rpm for 15 s using a spin coater after every dip-coating. Subsequently, the HA-

coated zirconia screw was coated with HA sol aged 3 days and heat-treated at 800 °C for 1 h at a heating rate of 5 °C/min. The precise description was the lower part of Figure 2.1.

2.3. Characterization of HA-coated zirconia

The surface microstructure of the HA-coated zirconia was analyzed using a field emission scanning electron microscope (FE-SEM; Supra 55VP, Carl Zeiss, Germany). Prior to the FE-SEM observation, a thin platinum layer was deposited (EM ACE200, Leica, Austria) to prevent electron charging. The aged HA sol was dried and observed through a Transmission electron microscope (TEM; Tecnai F20, FEI, USA). HA sol aged 1 day was used to confirm the HA particle. The viscosity of HA sol with various aging time was measured by rheology (DHR-2, TA instrument, USA) with a 20mm parallel-plate. Dynamic oscillatory frequency sweep was performed with constant strain over the frequency range of 10–100 rad/s. The crystal phase of the HA-coated zirconia was investigated by XRD (D8 advance, Bruker Miller co, Germany). Wide 2θ angle range of 20 °–60 ° and narrow 2θ angle range of 31 °–37 ° were obtained at a scan rate of 1 °/min because of its small intensity. The binding energy of HA-coated zirconia was measured by X-Ray Photoelectron Spectroscopy (XPS; AXIS-HSi, KRATOS, Japan). The focused ion beam (FIB,

Auriga, Zeiss, Germany) technique was used to analyze the coating layer thickness.

The mechanical stability of the coating layer was measured using the pull-out method. Epoxy precoated aluminum studs were placed on the coating surface and cured at 150 °C for 30 min. The stud was pulled from the attached surface at a rate of 1 mm/min using a universal testing machine (RB302 single-column type, R&B, Korea). Schematic image of measuring adhesion strength was presented at figure 2.2.

2.4. *In-vitro* osseointegration of the HA-coated zirconia

The initial cell attachment and proliferation were evaluated using preosteoblast cell lines (MC3T3-E1, ATCC, CRL-2593, USA). All specimens were sterilized with 70% ethanol solution and UV radiation prior to cell seeding. The pre-incubated preosteoblast cell lines were seeded on each sample at densities of 3×10^4 and 2×10^4 cells/ml for the cell attachment and proliferation assays, respectively. The cells were then incubated in a humidified incubator at 37 °C with 5% CO₂. The alpha-minimum essential medium (α-MEM, Welgene Co, Korea) containing 10% fetal bovine serum (Gibco, USA) and 1% penicillin-streptomycin (Pen strep, Gibco, USA) was used as the culturing medium for all tests.

The initial cell adhesion was observed using a confocal laser scanning microscope (SP8 X, Leica, Germany) 24 h after cell seeding. After fixing the attached cells with 4% paraformaldehyde solution, the cytoplasm and nuclei of the cells were stained with fluorescent phalloidin (Alexa Fluor® 555 phalloidin, Invitrogen, USA), and 4',6-diamidino-2-phenylindole (DAPI, Invitrogen, USA) and then observed using lasers with wavelengths of 540 and 350 nm, respectively.

The cell proliferation was assessed using the metoxyphenyl tetrazolium salt (MTS) method. A 10% reagent (CellTiter 96 Aqueous One Solution, Promega, USA) in culture medium was added to the cells on the specimens and incubated at 37 °C for 2h after 3 and 5 days of culturing. The supernatant absorbance was measured by a microplate reader (EZ read 400, Biochrom, UK) at 490 nm.

2.5. *In-vivo* osseointegration of the HA-coated zirconia

An animal test was conducted using a rabbit femoral defect model. This animal test was approved by Genoss's Institutional Animal Care and Use Committee. Twelve-week-old male New Zealand white rabbits with an average weight of 2.5–3 kg were anesthetized with 0.1 ml of 2% Xylazine HCl (Rompun, Bayer Korea, Korea) and 0.2 ml Tiletamine HCl (Zoletil, Virbac lab, France), and Lidocaine (Yuhan Corporation, Korea). A cylindrical defect with a radius of 0.9 mm was

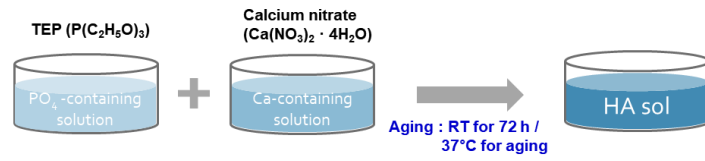
created on each leg. Zirconia and HA-coated zirconia screws and Ti screw, which are positive control, were then implanted to these defects by applying an insertion torque of 20 Ncm. A postoperative antibiotic, gentamicin (Dongkwang Pharmaceutical Co, Korea), was intramuscularly administered at 0.1 mg/kg for 3 days after surgery.

The rabbits were sacrificed four weeks after the surgery; further, the specimens were extracted from the surrounding tissues. For a histological observation, all the extracted specimens were immediately fixed with 10% formalin then embedded in resin (Technovit 7200 VLC, Germany). The resin blocks containing the specimen and the tissues were sliced to a thickness of 40 μ m. The slides were then stained using Goldner's trichrome method and observed using an optical microscope (Olympus BX51, Olympus, Japan). The osteoconductivity was evaluated in terms of the bone-to-implant contact (BIC) and new bone area ratios. The BIC ratio was calculated by dividing the length of the screw surface that bonded with the bone by the whole length of the screw surface. Additionally, the new bone area ratio was defined as the area of the newly generated bone relative to the area inside the threads at the top part of the screw.

2.6. Statistical analysis

Statistical Package for the Social Sciences (SPSS 23, SPSS Inc., USA) was used to perform the statistical analysis. All data were expressed as mean \pm standard deviation. The normality of the variables was verified using the Shapiro–Wilk test. The statistical analysis was performed by a one-way analysis of variance with Tukey post-hoc comparison. A p -value below 0.05 was considered significant in all cases.

1. HA sol manufacture



2. HA coating on zirconia using dip coating method

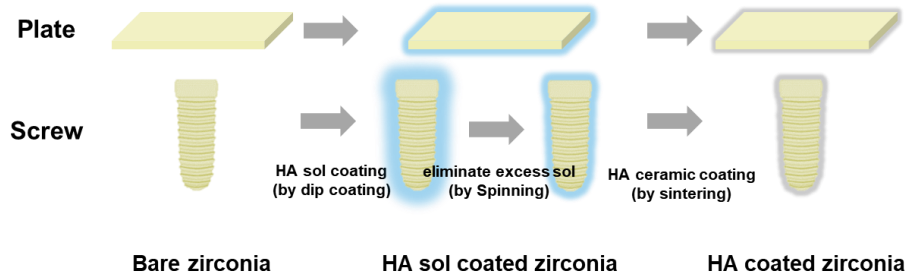


Figure 2.1. Schematic representation of experimental procedure

Table.2.1. Experimental conditions.

Variables		Experimental conditions
HA sol	Aging time	3h, 1d, 3d, 5d
Dip coating	Number	3 times
	Speed	0.25 mm/s
	Interval	5 min
	Spin speed (screw)	150 rpm
Sintering	Temperature	400, 600, 800, 1000 °C
	Time	1 h
	Heating rate	5 °C/m

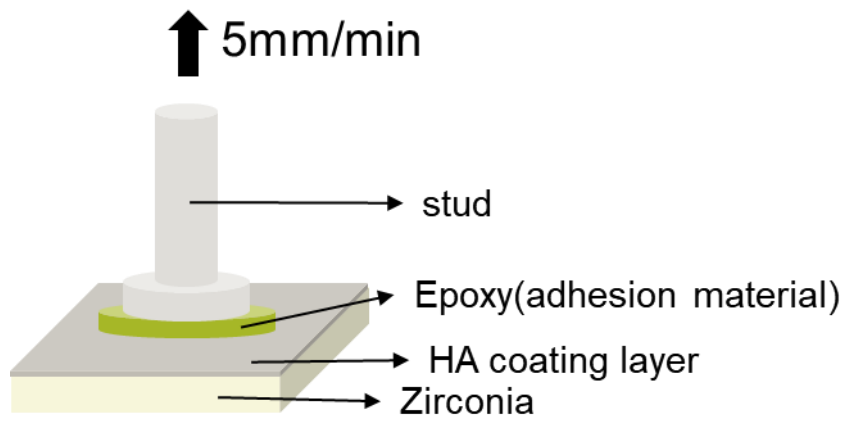


Figure.2.2. schematic images of adhesion strength test.

Chapter 3. Results and discussion

3.1. control the surface morphology of the HA layer

It was known that there were several factors that affect the surface roughness. In this paper, the purpose was to control nano- and micro-level roughness, and factors that could affect this were considered to be the sintering conditions of the HA layer and the properties of the HA sol itself. By controlling the sintering temperature and the aging time of HA sol, which could be adjusted, the change in surface roughness was checked.

3.1.1. sintering temperature

In order to control the surface roughness, it was necessary to find the factors affecting the surface roughness. The roughness was checked by observing the surface through SEM while changing the sintering temperature, which seem to be the most important cause. At this time, the HA sol was used under 3-day aging conditions. At a sintering temperature of 400 °C, the coating was not reliably achieved, at a sintering temperature of 600 °C, the nanoroughness was not observed well because the grain size was very small, and at a sintering temperature of 800 °C, a nano-level roughness was clearly observed. In all specimens, hydroxyapatite in the form of granules was observed in the coating layer, and it was confirmed that the size of hydroxyapatite gradually increased with temperature.

However, at 1000 °C, it was seen that the nano-sized grains became larger and flattened, reducing the roughness. Also, as the grains grow, the micro-level grains take on an angular shape, which was thought to interfere with the generation of a uniform roughness. If it was not uniform and the height difference was too large, it was difficult for the cells to attach widely to the surface, thus hindering the improvement of desired cellular response. Therefore, it was confirmed that the sintering temperature had an effect on the nano roughness. Below 600 °C, the grain size was too small, so the nano level roughness was not well confirmed. At a temperature of 1000 °C or more, the grain size increased and angularity occurred. It was confirmed that not only the nano-level roughness of the desired shape but also the micro-roughness could not be obtained. (figure 3.1.)

The morphological change of the HA coating layer at different sintering temperatures could be explained by the mobility of ions. As the sintering temperature increases, the mobility of ions also increases. The higher the mobility, the faster the reaction between the HA particles. For 600 °C sintering conditions, adjacent HA particles started to coalesce and form a granular structure on the zirconia surface. The porous structure at 800 °C sintering conditions could occur because the particle migration is not high enough to

create a dense surface. Similarly, at 1000 °C sintering conditions, most of the specimen surface was covered with a flat, dense layer of HA with large particle size due to high particle migration. In addition, pores were found on the inner HA layer and the surface of the HA layer, suggesting that they may have an interconnected structure. The microroughness of the implant surface was known to be highly correlated with the bone integrity of the material [66]. Based on these results, it was judged that the 800 °C sintering condition group has the highest bone conductivity due to the finely roughened surface.

By checking the structure of different surfaces according to the sintering temperature, it was possible to explain the increase in the particle size and the decrease in nano roughness at the sintering temperature of 1000 °C, but it was insufficient to explain the occurrence of micro roughness at the temperature of 800 °C or more. Therefore, it was found that the sintering temperature affects the nano roughness, but it was thought that the micro roughness is affected by other conditions.

3.1.2. HA sol aging time

Therefore, in order to find the cause of the micro-roughness, the sintering temperature was fixed at 800 °C, and then the aging time of

the hydroxyapatite sol itself was adjusted. (figure 3.2.) The microroughness was confirmed in the specimen using HA sol, and the crack layer was confirmed in the specimen using HA sol aged for 5 days. At the enlarged picture, clear difference was confirmed. Specimens using HA sol aged for 3 hours could confirm that the coating layer is not evenly coated because the aging time was too short to generate much HA particles. The structure of the substrate, zirconia, had been confirmed without being evenly coated. However, in the specimen using HA sol aged for 1 day, no micro-level roughness was observed, and a coating layer having only very uniform nano-roughness was formed. On the other hand, in the specimen using the HA sol aged for 3 days, there was a coating layer with the same nano-roughness as in the specimen using the HA sol aged for 1 day, and micro-level roughness having a size of about 2 μm was confirmed thereon. Therefore, it was possible to form specimens having both nano- and micro-level roughness under these conditions. On the other hand, in the specimen using HA sol aged for 5 days, the coating layer became too thick due to the formation of excessive HA sol, and cracks appeared in the coating layer.

To find the cause of this phenomenon, hydroxyapatite sol was dried and observed through TEM. (Figure 3.3.) It could be confirmed that very small-sized particles exist in all types of TEM images. Among

them, the HA sol aged for 3 hours and the HA sol aged for 1 day were dried and confirmed, no particles exceeding 10 nm were generated. It seems that the particles generated through the nucleation and growth process in the sol-gel method are observed. However, in the images of HA sol aged for 3 days and HA sol aged for 5 days, it was confirmed that particles with a size of 100 nm or larger were formed. And it was also confirmed that the size of the particles increases as the aging time increases from 3 days to 5 days. It was considered to be a phenomenon caused by secondary growth due to sufficient aging time in the sol-gel method. As small particles agglomerate each other through aging and increase in size, relatively very large particles are formed. Therefore, small particles form nano roughness, and particles grown by secondary growth create micro roughness. Through this, it could be considered that the aging time of the hydroxyapatite sol affects the particle size inside the sol and affects the roughness of the coated surface.

Additionally, to confirm that the particles formed at this time were HA particles, the TEM image observed using the HA sol aged for 1 day and the interplanar distance and interplanar angle in the FFT image were checked. group could be confirmed (Figure 3.4.). The large particles in the HA sol aged for 3 days or more could not be observed because they were too thick to confirm the crystallinity,

but considering that the above-mentioned particles are agglomerated and formed, it could be considered that these are also HA particles. Although the crystallinity was not clearly confirmed, this was because sintering has not been performed yet, and only the sol-gel method is confirmed. Therefore, confirmation of such crystallinity was confirmed once again by observing through another method after sintering is completed.

In addition, an excessive level of aging time made the coating layer thick, and cracks were observed in the specimens using HA sol aged for 5 days. This was the part that can be confirmed through the viscosity shown in figure 3.5. From this, it was confirmed that the specimen produced with HA sol has a much larger viscosity than the solvent ethanol. In the case of ethanol, the average viscosity was 0.00068 Pa·S, whereas in the case of other specimens, the HA sol aged for 3 hours has a minimum value of 0.00175 Pa·S. And the viscosity was increased as the aging time of the specimen increase. Compared to other HA sols with similar values (0.00181 and 0.00182 Pa S aged for 1 day and 3 days, respectively), the HA sol aged for 5 days was 0.00190 Pa. It was thought that there was a significant difference with the value of S. and D.B. According to HADDOW et al., the thickness of the coating layer was known to be affected by viscosity, and therefore, when coated with HA sol aged for 5 days,

which has a fairly large difference, the thickness was excessively thick and cracks appear [67].

3.2. Control the reaction of HA and zirconia by adjusting sintering temperature

3.2.1. Characteristics of HA coated zirconia with various sintering temperature

The crystalline phases of the HA layers with different sintering temperatures were investigated by XRD to know and control the conditions under which byproduct occur (Figure 3.6.). At this measurement, Aging time of HA sol was 3d, because it is a condition that can adjust the surface structure. Since the coating layer was formed very thin, in the xrd image (Figure 3.6.(a)) measured in a wide range (20–60°), the characteristic peak of zirconia was observed too large, and the peaks of other components could not be confirmed. Therefore, it was measured in a narrow range (31–37°) in which the peaks of hydroxyapatite and calcium zirconate were observed, and the result is shown in figure 3.6.(b). Two main peaks on the bare zirconia substrate (ICDD data file no. 01-072-2743) were detected at 34.7° and 35.3°, which corresponded to the (110) and (002) planes of tetragonal zirconia, respectively. A broad and

small peak corresponding to the (200) plane of cubic zirconia was detected at around 35° [68]. The XRD pattern of sample which sintered at 400°C also demonstrated the characteristic peaks of zirconia but did not show any calcium phosphate peak. The HA peaks (ICDD data file no. 04-014-8416) began to be detected at 31.9° , 32.2° , and 33° corresponding to (211), (112) and (300) planes, respectively, when the sintering temperature was above 600°C [69]. The intensity of the HA peaks also increased when the sintering temperature increased. However, for specimen which sintered at 1000°C , aside from the sharper and higher HA peaks, calcium zirconate phase (ICDD data file no. 04-001-9308) was also detected at 31.7° [70]. Analysis of the crystallinity of HA coated zirconia revealed more information. The absence of any peaks in XRD observations means that the HA layer does not crystallize at sintering temperature conditions as low as 400°C . Amorphous HA has a very high dissolution rate; hence, sintering at 400°C would not be appropriate for the coating purpose to improve the osseointegration of dental implants [71]. Calcium zirconate observed in XRD analysis of specimens fabricated at a sintering temperature of 1000°C is an undesirable reactant of HA and zirconia because it consumes calcium and reduces the Ca and P ratio in the calcium phosphate.

In order to check the production of by-products more specifically, the binding energy was measured through XPS. All the specimens were not observed, and by comparing the 800 °C sintering temperature which is the highest sintering temperature at which calcium zirconate was not formed and the 1000 °C sintering temperature at which calcium zirconate was observed, it was attempted to determine whether calcium zirconate was formed. The image obtained by measuring the binding energy of HA coated zirconia sintered at 800 °C and 1000 °C through XPS is shown in figure 3.7. The xps only checks the thin thickness of the surface of about 10 nm. Therefore, only the elements of the coating layer can be observed in XPS. Accordingly, only the constituent elements constituting HA such as O, Ca, and P are observed in the specimen with 800°C sintering temperature. Unlike the specimen sintered at 800 °C (figure 3.7.(a)), zirconium is observed in the case of the specimen sintered at 1000 °C (figure 3.7.(b)) [72, 73]. This means that a material containing Zr was produced in the coating layer, and when referring to the above XRD data, it can be expected that it is calcium zirconate. In addition, looking at the binding energy of oxygen, in the specimen sintered at 800°C, only binding energy in phosphoric acid and hydroxyl groups in HA observed at about 531 eV is observed. However, in the specimen sintered at 1000 °C, the

binding energy of the metal oxide was observed at about 529 eV, which is considered to be the binding energy of Zr-O bonding in the situation where Zr is observed and calcium zirconate is generated. (figure 3.7.(d)) [74].

These results suggest that the HA coating layer should be heat-treated at a temperature between 400 °C and 1000 °C to obtain the crystalline HA phase without any by-products. If it exceeds 1000 °C, by-products are formed, and below 400 °C, HA does not crystallize much. Based on this, the optimum temperature can be said to be 800 °C, the highest temperature at which no by-products are produced.

3.2.2. Coating stability of HA coated zirconia

After the peel-off test, the failed region was investigated using SEM observation (Figures 3.8.). Figure 3.9. shows the adhesion strength of HA layers examined by peel-off test, which is widely used to evaluate the adhesion strength of HA coating layer [64, 75, 76]. Bare zirconia also measured under the same conditions to determine the bonding strength of stud and epoxy. HA coated zirconia which sintered at 400 °C was excluded because it was not suitable for coating purpose, because the specimen sintered at 400 °C has a very low crystallinity, so it is difficult to say that it is HA. All sample

groups demonstrated the adhesion strength higher than 50 MPa without a statistical difference. In particular, the fact that it shows a value of about 50 MPa even in a bare specimen without a coating layer suggests that this number is the adhesion between the epoxy and the stud. For all specimen surfaces, epoxy resin remained on the most of surface, and delamination of HA layer was not observed even epoxy resin was removed. Therefore, it is considered that the measured value is the adhesion between the epoxy and the stud. However, the specimen sintered at 1000 °C shows a slightly different pattern. Although the measured adhesion strength is not a significant difference, it shows a slightly small value of about 40 MPa. And when the surface from which the epoxy was peeled off (figure 3.8.(d)), all the grains that make up the micro-roughness came off, and the HA coating layer was also observed. It is thought that the calcium zircoante formation reaction above 1000 °C also affected the stability of the coating layer.

The mechanical stability of the coating layer is a very important factor for the success of the implantation. The coating layer is not effective anymore if it is peeled off during the surgery. Additionally, delaminated debris could induce unwanted bone regeneration [77]. Weak bonding strength between coating and substrate also can cause micromovement of implant which might result in implant failure [78,

79]. From this point of view, the adhesion strength measured by the peel off test shows that the mechanical stability of the HA coating could be reasonable for dental applications. The measured strength must be lower than the actual adhesion strength between the HA layer and zirconia substrates because the separation of the HA layer is not seen when observing the area after measurement. In this way, several existing studies have measured the coating strength of various materials, which is similar to or lower than the value of 40 MPa in this study [80–82]. According to ISO standard (ISO 13779) and researches, adhesion strength higher than 15 MPa is considered acceptable [76]. In addition, it was confirmed that the bonding strength measured in a similar method in the previous papers on HA coated zirconia sintered at a high temperature of 1600 °C has a value of 11.68 MPa [83, 84]. This was thought to be a phenomenon caused by the decrease in mechanical properties due to the formation of TCP and calcium zirconate at high temperatures mentioned above, and this was proved through the observation of TCP in XRD analysis of the fracture surface. Therefore, HA coated zirconia obtained through sintering at a relatively low temperature had a bonding strength superior to existing studies as well as international standards, making it suitable for implant application. Collectively, 800 °C was chosen as the optimum sintering temperature for further

biological test because HA800 showed the most ideal characteristics in terms of surface morphology, crystallinity, and coating stability.

Therefore, since the measured adhesion strength value is sufficiently large, it is suitable for use as a coating layer under all measured sintering temperature conditions. However, it is confirmed that the adhesion of the grains constituting the micro-roughness is lowered under the sintering temperature condition of 1000°C or higher in which calcium zirconate is produced, and the stability of the coating layer is also lowered, so it is not suitable.

3.3. Comparison of HA-coated zirconia with and without micro roughness

From now on, based on the previous results, the temperature condition was fixed at 800 °C, which was stable because no by-products were generated and the crystallinity was the highest. Since it was possible to control the roughness of the hydroxyapatite-coated zirconia surface, a specimen having only nano roughness was made using a solution aged for 1 day, and a specimen having nano and micro roughness was made using a solution aged for 3 days.

First, it was checked the thickness of the coating layer through FIB and checked the inside to see if the micro-roughness part was not

empty and the coating layer was stable even inside (figure 3.10.). It was confirmed that the surface with nano-roughness formed a thin coating layer of approximately 200 nm, which formed the desired thin and stable HA thickness layer in this experiment. And this thickness was much thinner than in the previous studies [8, 75]. On the other hand, it was confirmed that the surface with micro-roughness had a thickness of about 800 nm. And the size of the grains constituting the roughness could also be confirmed more clearly. And the size of the grains constituting the roughness could be confirmed more clearly. Since the size of the grains constituting the nano-roughness were about 50 nm, and the grains having the micro-roughness were about 800 nm, it was possible to have nano- and micro-level roughness. It was possible to check the inside of the particles making up the micro-roughness, and it was not empty and had a porous structure even inside. Therefore, it was also able to prove that this structure was formed from the agglomerated particles of HA sol, not from delamination or failure that occurred during sintering or coating.

Next, the roughness level of the two specimens was checked through the 3d surface profile (figure 3.11.). There was a clear difference in the photos. The overall roughness of the specimen using HA sol aged for 3 days was confirmed, whereas the specimen

using HA sol aged for 1 day had no micro-roughness when checked on the same scale. Looking at the graph of quantitative roughness measurement (figure 3.11.(c)), the two specimens showed a clear difference in both Rq and Ra. When comparing only the Rq value, it was confirmed that the specimen aged for 1 day had a roughness of about 100 nm and the specimen aged for 3 days had a roughness of about 350 nm. This was a result that was somewhat consistent with the difference in thickness compared to the one-day aging specimen, although it showed a larger value than expected due to the defect of zirconia itself.

Next, XRD analysis was performed to confirm that all specimens with different surface structures made by controlling the aging time had the same CaP phase (figure 3.12.). As when checking the XRD specimen according to the sintering temperature, the peak of zirconia was too large at 20-60°, so it was confirmed in the range of 31-36° where the calcium phosphate phase was confirmed. The reason for confirming this was that if the aging time is increased, substances having a different phase of calcium phosphate other than HA might be formed. As a result, no phases other than hydroxyapatite and zirconia were detected in specimens using HA sol with aging times of 1 day and 3 days, confirming that stable hydroxyapatite was well produced in all specimens. And the longer the aging time, the clearer

the peak, which mean that the amount of HA in the HA sol increased and the crystallization improved.

3.4. *In-vitro* osseointegration of the HA-coated zirconia

It was confirmed that the surface morphology could be controlled by controlling the HA sol aging time and the sintering temperature, as well as a stable coating layer without by-products could be formed. Under 800 °C sintering conditions, no by-products were formed and a surface structure with nano level roughness could be made, and micro roughness could be controlled by dividing the aging time of HA sol into 1 day and 3 days, respectively. Therefore, in this part, the osteocompatibility of HA-coated zirconia was to be confirmed using osteoblasts. First, the difference in bone compatibility due to the presence or absence of micro-roughness was checked, and the cellular characteristics of HA coated zirconia and uncoated zirconia produced under conditions of better bone compatibility, and the most widely used titanium were tried to be verified.

3.4.1. osteoconductivity of roughness difference

Based on these results, it was possible to control the surface structure of the stable hydroxyapatite coating layer, so it was possibly checked the initial osteosynthesis. First, it was checked the

degree of cell adhesion through SEM (figure 3.13.). Observations were made over periods of 3 and 24 hours. When the specimen with only nano-roughness was observed, it was confirmed that the cells stretch out in all directions, but the extension of cells was not large. On the other hand, when looking at the specimens with nano and micro roughness, it was confirmed that the cells were extending to the part with micro roughness, and it was confirmed that they were closer to the surface of the specimen. Clearly, early cell adhesion was affected by roughness.

At the same time, the initial osteosynthesis was confirmed again through CLSM (figure 3.14.). As with the previous SEM images, cells stretched better on specimens with micro-roughness and poorly on specimens that did not. Comparing the area covered by cells by confirming this statistically, the specimen with micro-roughness covered about 50%, but the specimen without micro-roughness covered only 15% or less. From this, it could be said that the specimen with micro-roughness has better initial osseointegrability.

3.4.2. osteoconductivity of HA coated zirconia

Based on the above results, a specimen aged 3 days with hydroxyapatite sol and sintered at 800 °C was considered the most ideal dental implant, so it was set this condition to hydroxyapatite-

coated zirconia and conducted a cell experiment. At this time, for comparison, titanium, which was currently most widely used, was set as a comparison group, and zirconia and hydroxyapatite-coated zirconia were set as an experimental group [17]. Looking at the images observed by CLSM of cell adhesion, it was confirmed that the cells were stretched very widely in titanium, and the cells of HA-coated zirconia showed a similar pattern, whereas in zirconia, the cells did not stretch well (figure 3.15.). This was mainly due to the zirconia properties known as bioinert [85, 86]. In the table after calculating the area covered by cells, the hydroxyapatite-coated zirconia shows a marked increase compared to the uncoated zirconia. As a result of confirming the degree of proliferation, titanium and hydroxyapatite-coated zirconia showed the same level of proliferation in the specimen cultured for 5 days, unlike zirconia (figure 3.16.).

3.5. *In-vivo* osseointegration of the HA-coated zirconia

The following were the results of an animal experiment. It could be seen the black titanium implant and the gray zirconia implant (figure 3.17.). At the enlarged image, it was observed that in the case of titanium and HA coated zirconia, there was a blue visible bone tissue surrounding the implant. However, in the case of zirconia, it could be

seen that the surrounding bone cells hardly touched the specimen. In particular, almost no new bone tissue with a slightly darker blue color was formed around the zirconia. Osteoblasts migrated around the implant to restore damaged tissue, but they did not come into contact with zirconia with poor cell properties, and contact well with hydroxyapatite-coated zirconia to improve cell properties. By quantitatively analyzing this, the bone-implant contact ratio (BIC) and the area of bone tissue around the implant were calculated. (figure 3.18.) Zirconia coated with hydroxyapatite has approximately 50% of the bone-implant contact ratio and 50% of the surrounding bone tissue area, which was similar to titanium, which was known to have good cellular properties, while uncoated zirconia BIC was 10% and the area of surrounding bone tissue was 30%, showing a clear difference. In animal experiments, it was confirmed that coating hydroxyapatite on zirconia can increase cellular properties to a level similar to titanium.

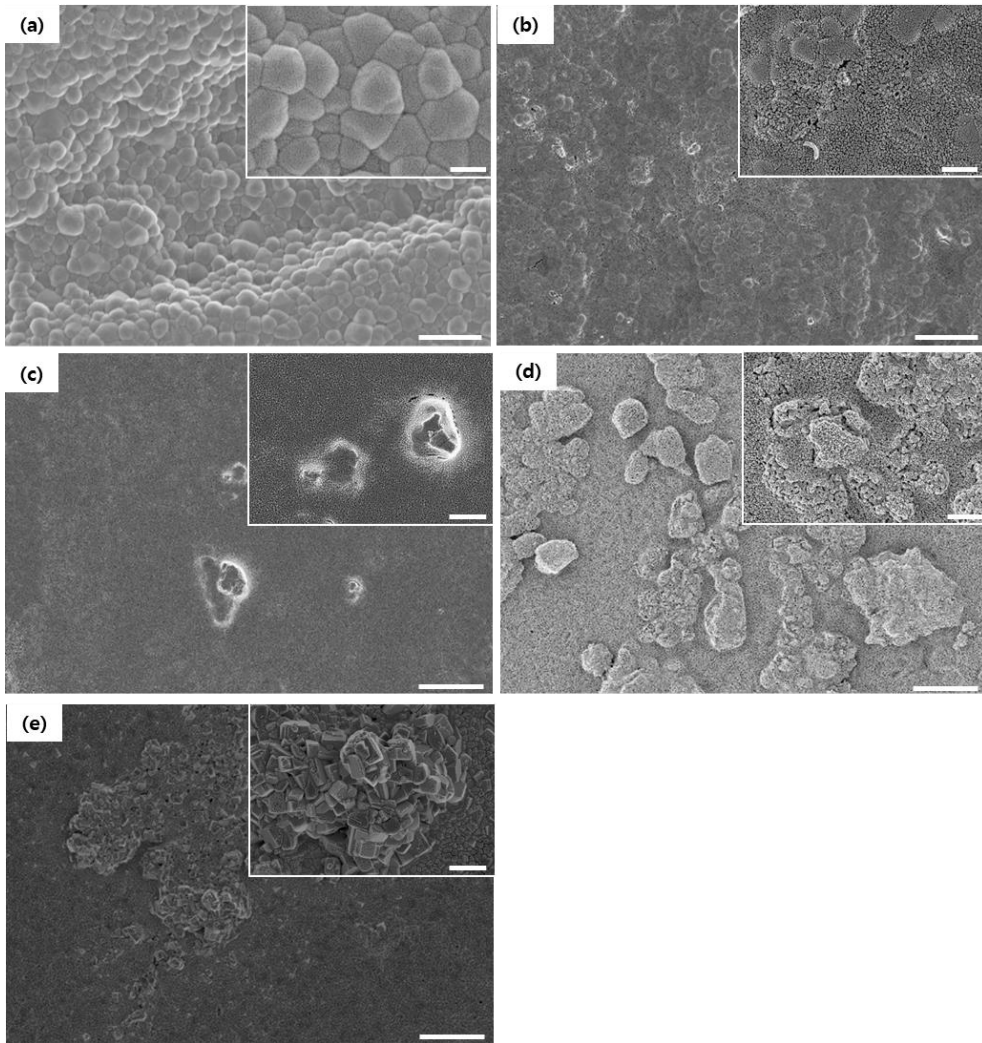


Figure.3.1. surface morphology of HA coated zirconia which sintered at various temperature; (a) bare, (b) 400 °C, (c) 600 °C, (d) 800 °C, (e) 1000 °C

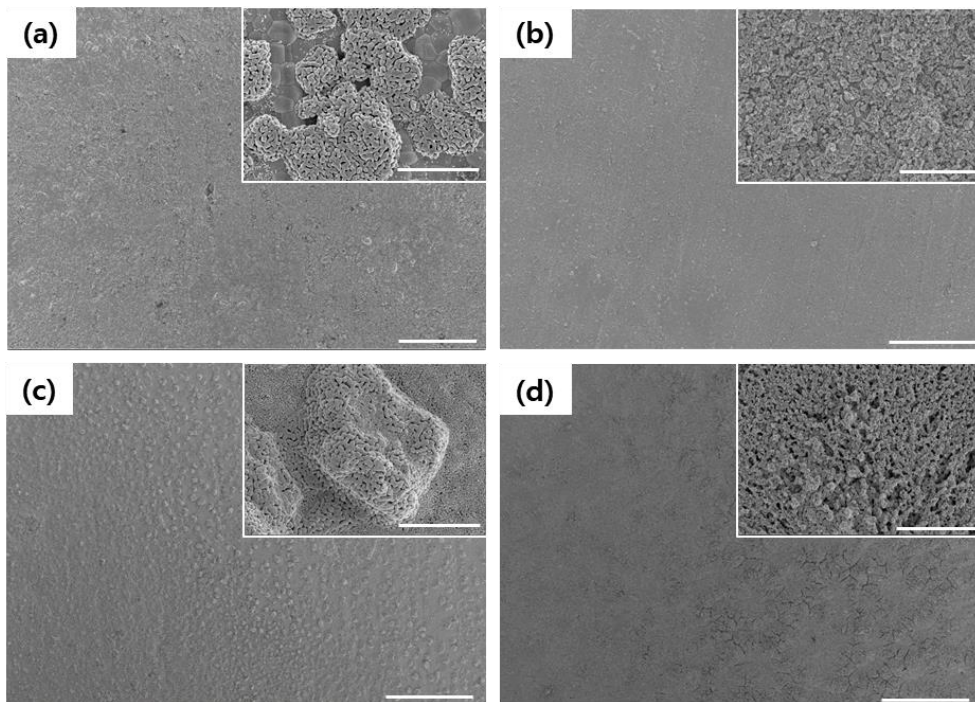


Figure.3.2. surface morphology of HA coated zirconia with various HA sol aging time, (a) 3h, (b) 1d, (c) 3d, (d) 5d. Scale bar: 50 μm (large), 2 μm (inset)

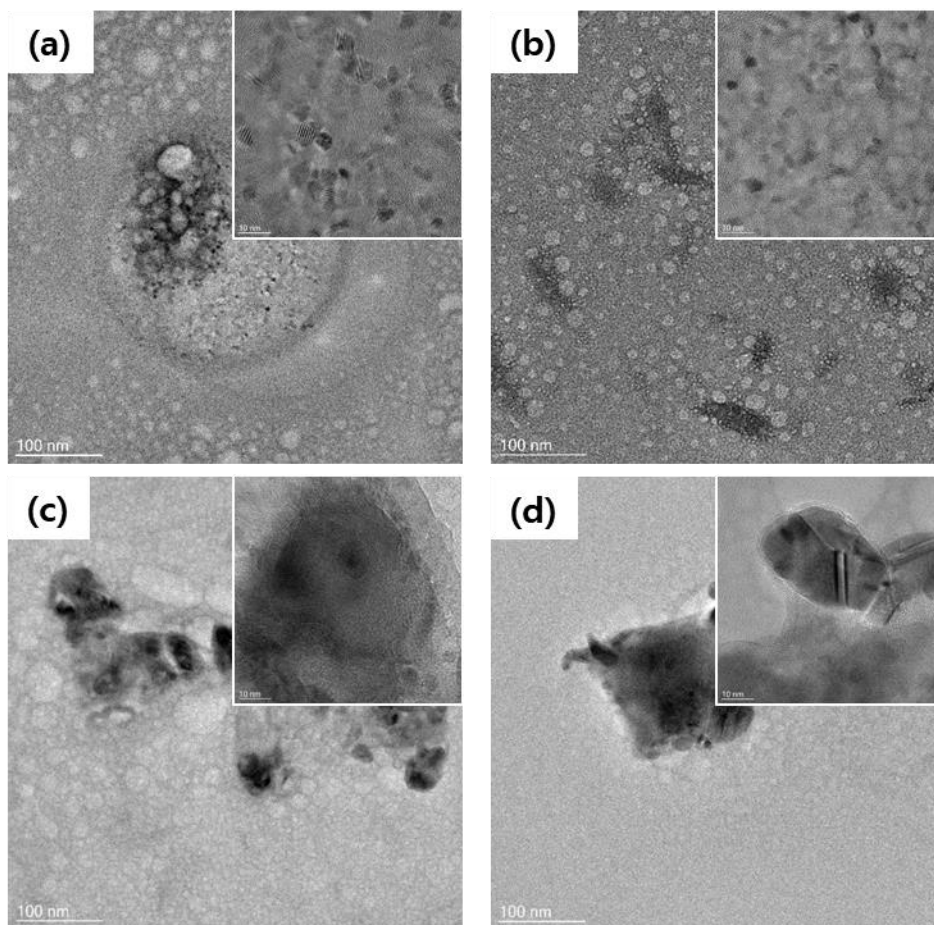


Figure.3.3. TEM images of dried HA sol with various aging time, (a) 3h, (b) 1d, (c) 3d, (d) 5d. Scale bar: 100 nm(large), 10 nm(inset)

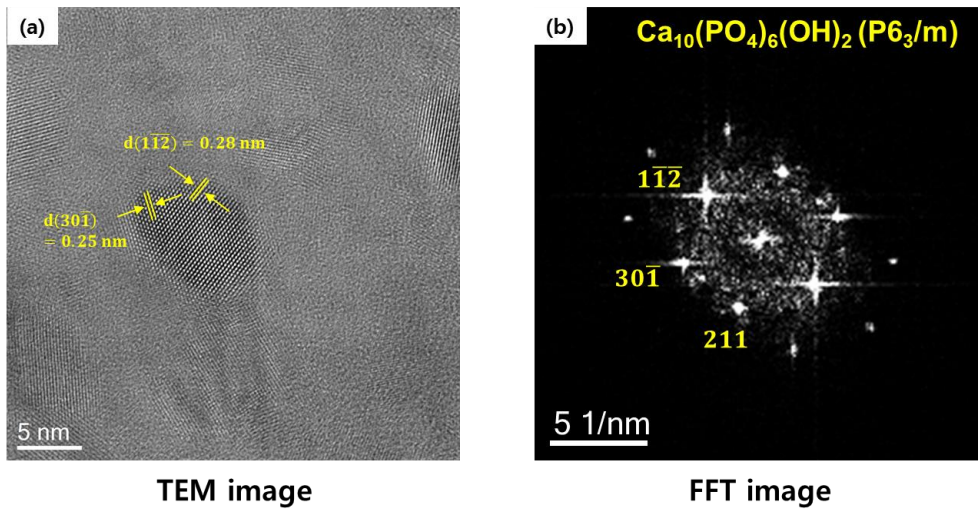


Figure.3.4. (a) TEM image and (b) FFT image of dried 1d aging HA sol.

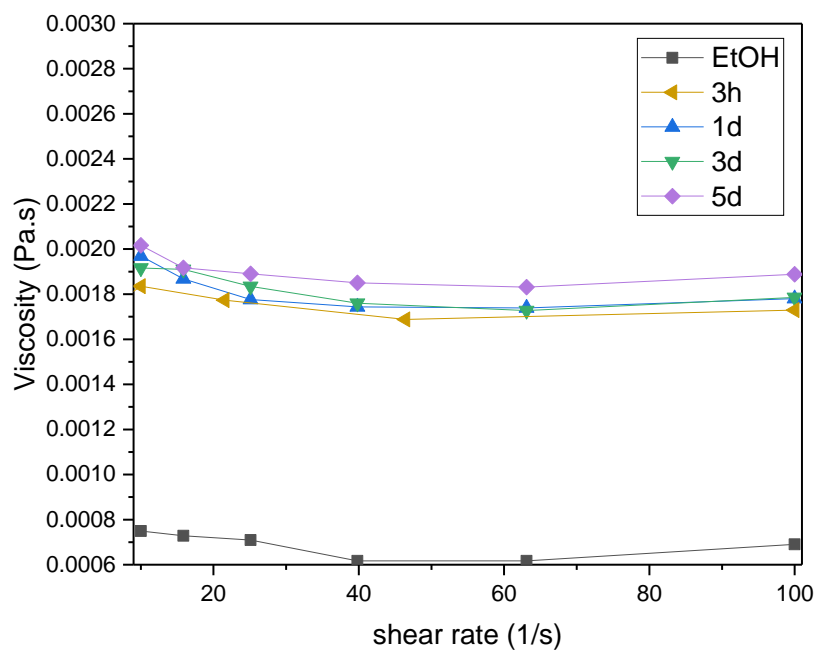


Figure 3.5. Viscosity of HA sol with various aging time and Ethanol (solvent).

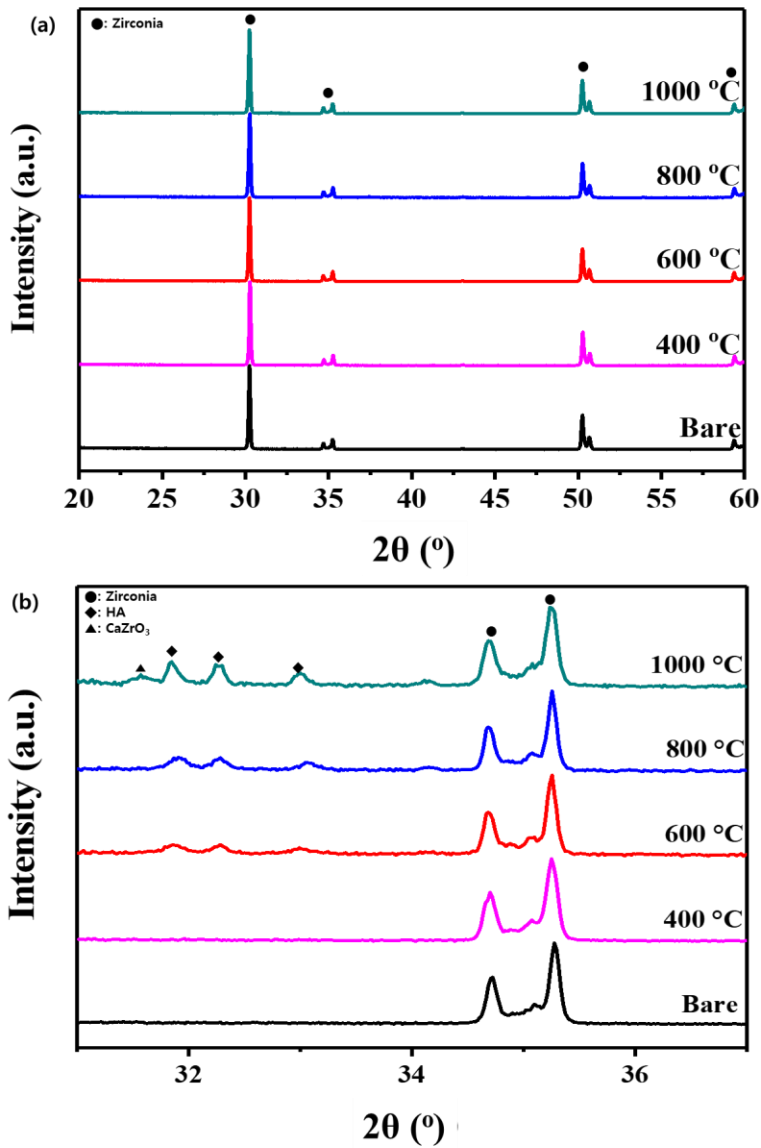


Figure.3.6. XRD patterns of the HA-coated zirconia substrates with various sintering temperatures; 2θ range of 20 – 60 degree (a), 31– 37 degree (b)

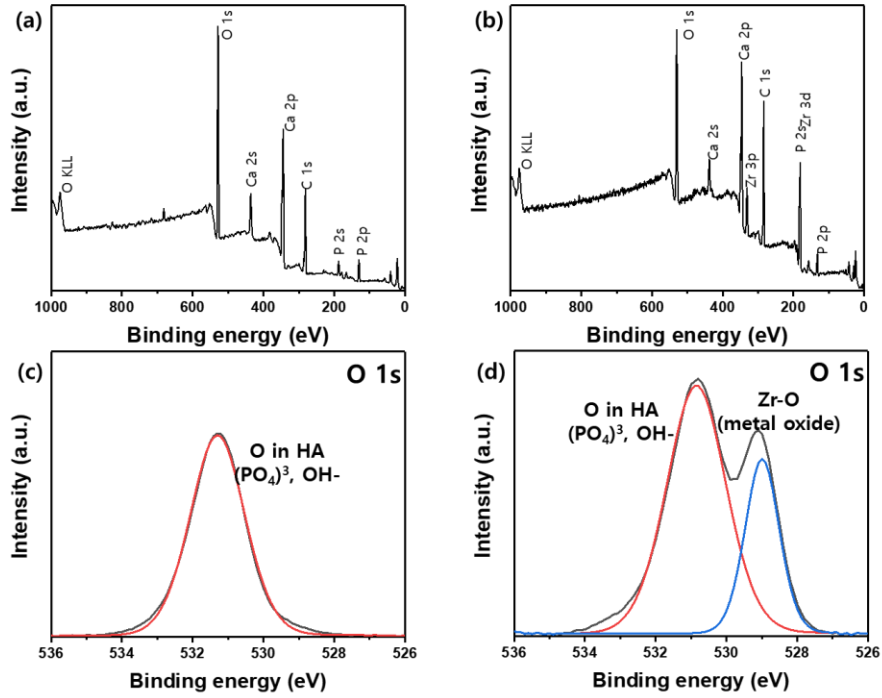


Figure 3.7. XPS data of HA-coated zirconia substrates with 800 °C (a) and 1000 °C (b) sintering temperature and Oxygen binding energy of 800 °C (c) and 1000 °C (d).

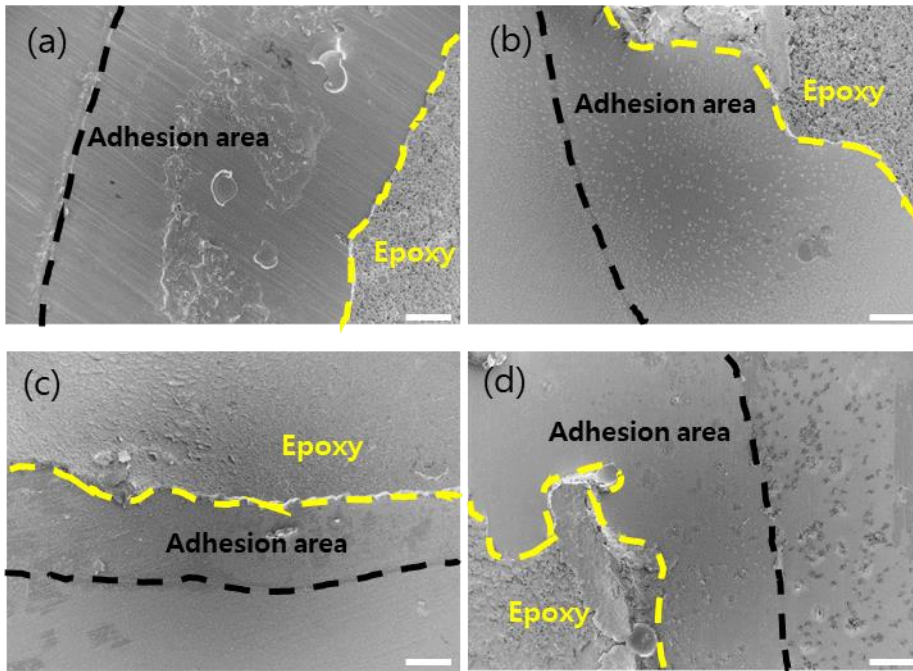


Figure 3.8. SEM images of the failure surfaces of the bare and HA-coated zirconia after the adhesion test: (a) bare zirconia, (b) HA600, (c) HA800, and (d) HA1000. The black and yellow dotted lines indicate the areas where the stud adheres to and epoxy remains, respectively. Scale bars: 500 nm.

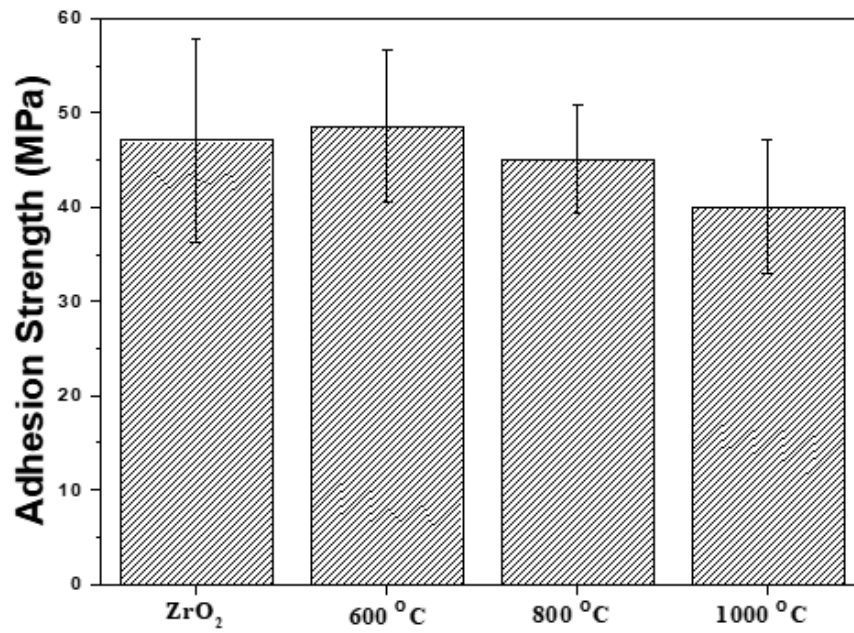


Figure.3.9. Adhesion strength of the HA-coated zirconia substrates with various sintering temperatures.

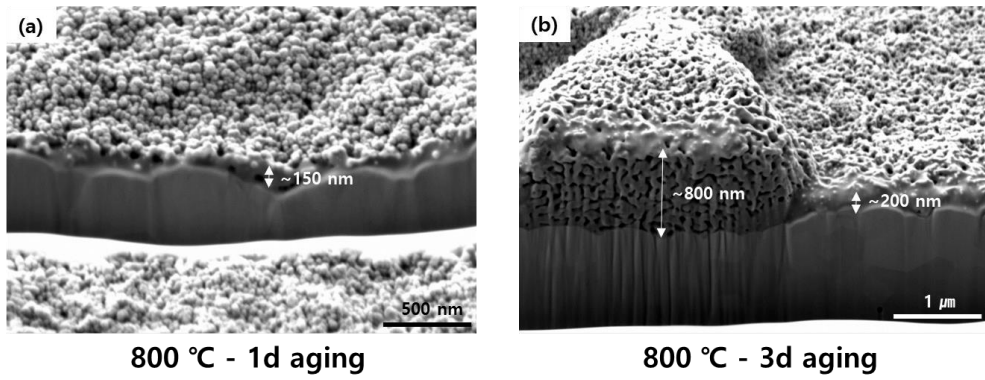


Figure.3.10. Thickness of HA coated zirconia using 1d aging HA sol (a) and 3d aging HA sol (b)

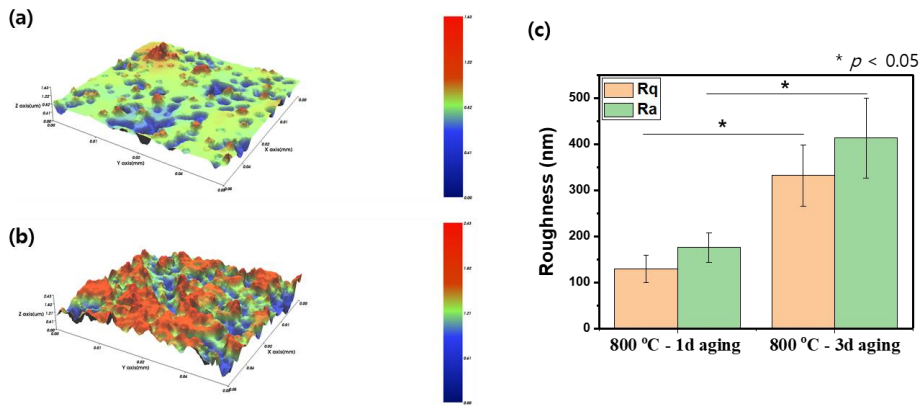


Figure.3.11. Surface roughness of HA coated zirconia using 1d aging HA sol (a) and 3d aging HA sol (b). Rq and Ra value of HA coated zirconia (c).

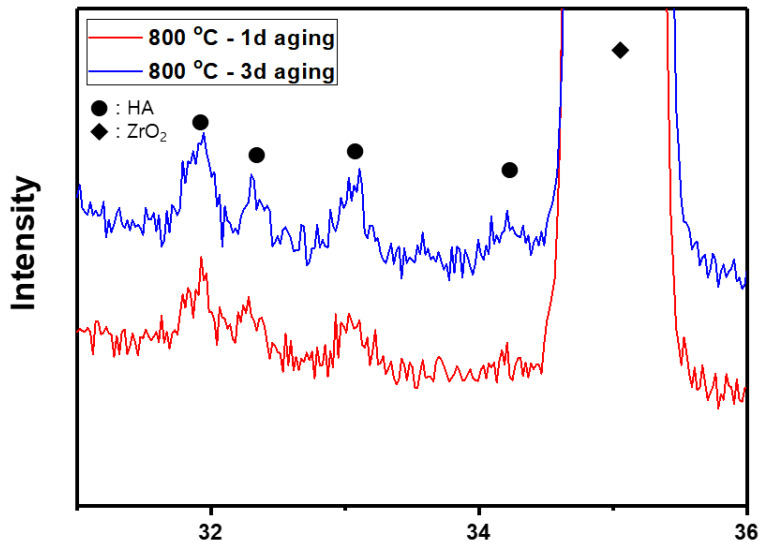


Figure.3.12. XRD analysis of HA coated zirconia using 1d aging HA sol and 3d aging HA sol.

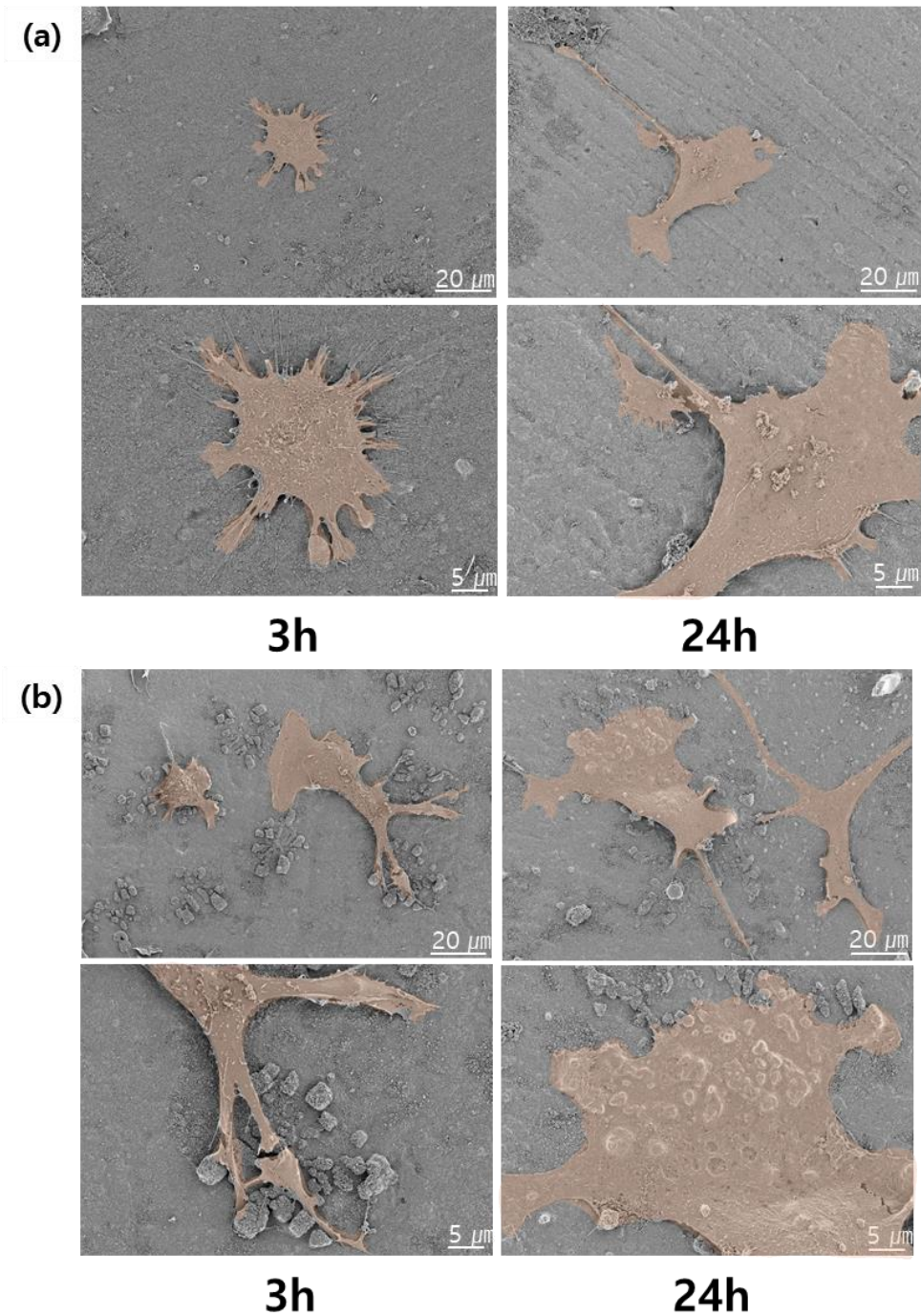


Figure.3.13. SEM images of cells attached on the HA coated zirconia using 1d aging HA sol (a) and 3d aging HA sol (b).

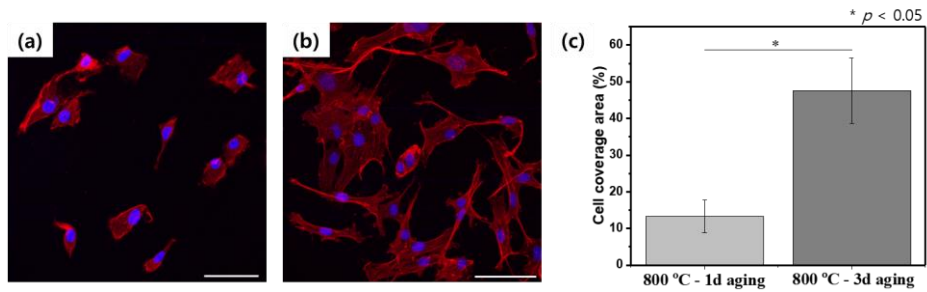


Figure.3.14. Confocal laser scanning microscope image of the cells attached on the HA coated zirconia using 1d aging HA sol (a) and 3d aging HA sol (b) and cell coverage area (c). Scale bars: confocal image (20 μ m).

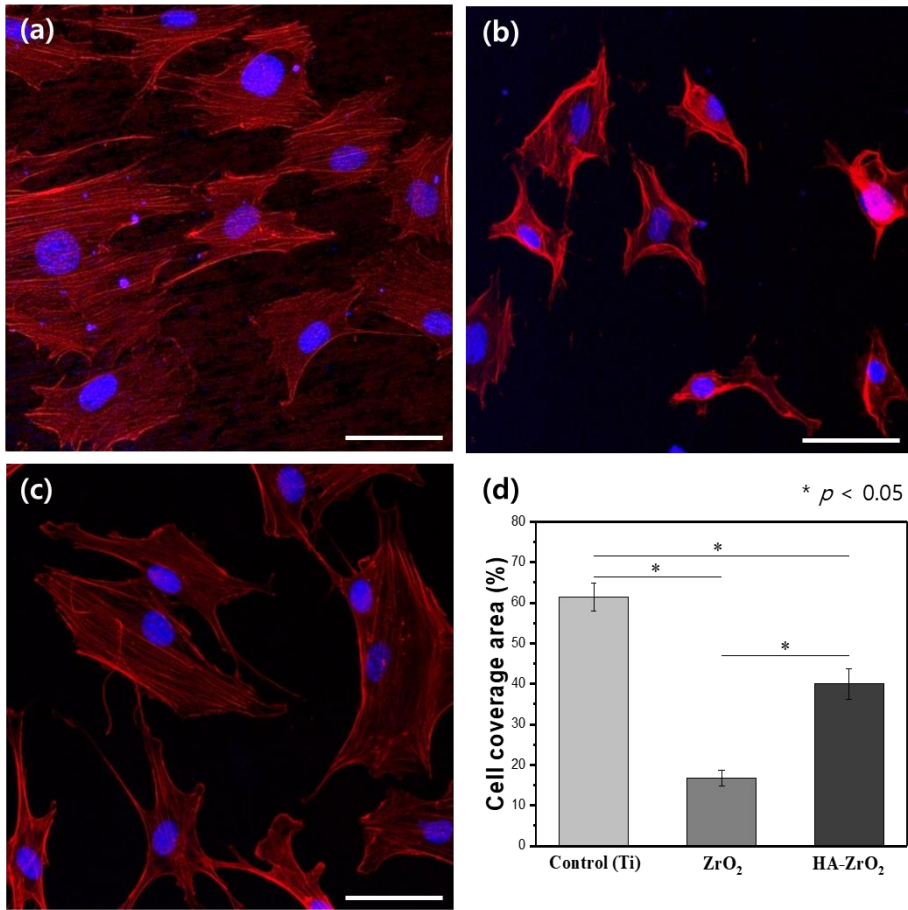


Figure.3.15. Confocal laser scanning microscope image of cells attached on the (a) Ti, (b) bare, and (c) HA-coated zirconia surfaces with cell coverage area (d). Scale bars: confocal image (20 μ m).

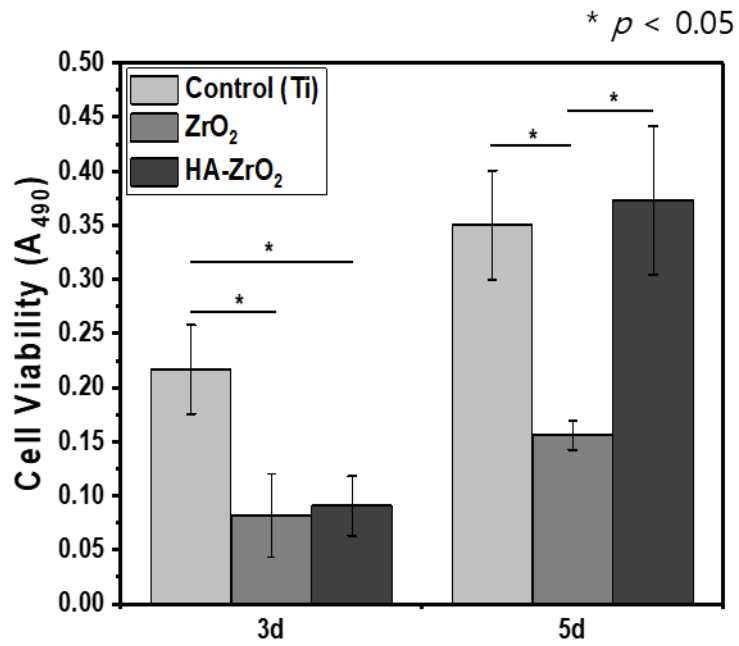


Figure 3.16. Degree of proliferation of the MC3T3-E1 cells on the Ti, bare, and HA-coated zirconia substrates after 3 and 5 days of seeding

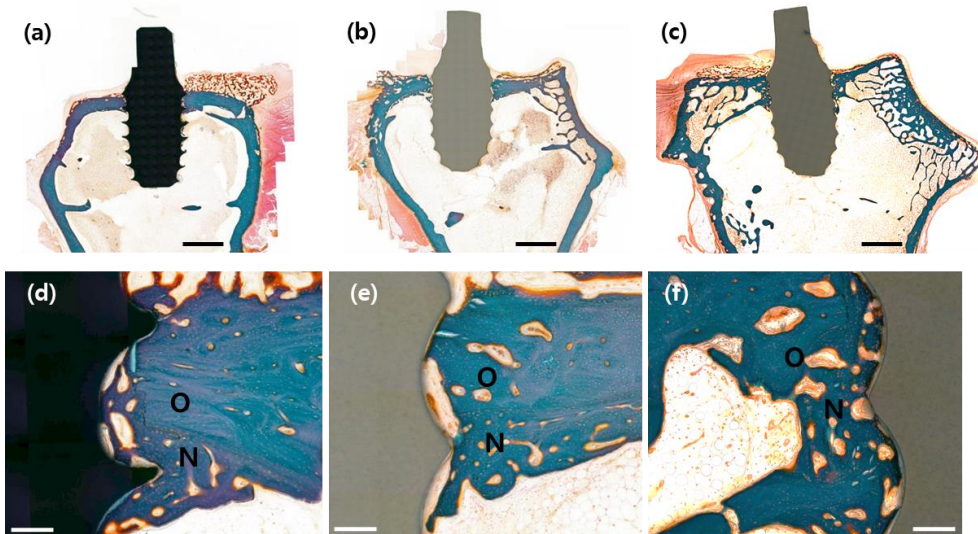


Figure 3.17. Representative histological cross-sectional image of the stained slices after 6 weeks of implantation: (a, d) Ti, (b, e) bare, and (c, f) HA-coated zirconia. O and N indicate the old and new bone areas, respectively. Scale bars: (a–c) low-magnification image (2 mm) and (d–f) high magnification images (200 μm).

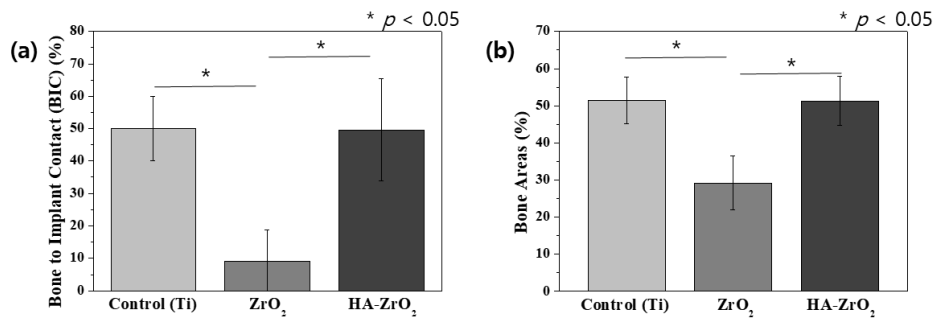


Figure 3.18. (a) Bone-to-implant contact and (b) new bone area ratios of Ti, bare-, and HA-coated zirconia.

Chapter 4. Conclusions

4.1. Conclusions

Herein, in a world where life expectancy is increasing, dental health and maintenance is a very important part. Since teeth can be lost for various reasons and cannot be regenerated, a dental implant to replace them is considered to be more essential than anything else. Titanium implants, which are most commonly used, have excellent bio-properties and physical properties, but disadvantages such as aesthetic disadvantages, metal-specific immune response and corrosion risk, and rare allergic reactions are highlighted.

In this trend, the demand for using zirconia, a ceramic with excellent physical properties, as a dental implant is increasing. In a situation in which various methods are being treated to increase insufficient bio-properties, a coating method using HA is being considered. Although HA is coated on zirconia by various methods, each coating method has its own advantages and disadvantages. The most important part is the stability of the coating layer, which is greatly affected by the thickness of the coating layer and the generation of by-products. To solve this problem, the method selected in this study is the dip coating method using the sol-gel method that can form the thinnest coating layer.

The main purpose of this study is to control the surface structure to further increase bone compatibility and the fact that the phase

change temperature of HA to TCP, which is a problem in the zirconia coating method using the sol-gel method, is significantly lowered by the reaction with zirconia. To this end, we tried to check the effect by controlling the aging time and sintering temperature of HA sol, and we tried to check the difference in cell characteristics by controlling the surface structure as well. Finally, HA-coated zirconia, zirconia, and widely used titanium will be compared in vitro and in vivo to confirm bone compatibility.

First, it was checked whether the surface structure could be controlled by adjusting the sintering temperature and the aging time of HA sol. When the surface structure was confirmed through SEM, nano roughness was controlled by sintering temperature and micro roughness was controlled by aging time. At 800 degrees Celsius or higher, nano roughness is generated, but at 1000 degrees Celsius or more, the nano roughness is rather lost due to the too large particles. When the aging time was 1 day, only uniform nano roughness was generated, and when the aging time was 3 days, micro roughness was generated. The reason was found by confirming that growth including secondary growth occurred through TEM. In addition, the thickening of the coating layer was confirmed by measuring the viscosity.

And when the sintering temperature was over 1000 degrees, the

formation of calcium zirconate, a by-product, was confirmed through XRD and XPS, and the adhesion test also affected the stability of the coating layer. In conclusion, sintering at 800 degrees was the condition to form a stable coating layer with crystallinity and no by-products.

The most stable sintering temperature was known, and in order to check the difference depending on the presence or absence of microroughness, specimens were manufactured using the condition that the aging time of HA sol was 1 day and 3 days. By checking the thickness and roughness, it was confirmed that the specimen with micro-roughness had greater roughness than the specimen with only nano-roughness. And by measuring XRD again, it could be seen that there was no difference in the composition according to the aging time.

Based on the above results, the difference in cell characteristics according to the presence or absence of microroughness was confirmed by measuring the degree of cell adhesion using osteoblast cells and SEM and CLSM. Through this, it was found that bone compatibility increased when micro-roughness was present.

In conclusion, HA sol aged for 3 days with micro-roughness was used and compared with other materials. It was compared with the zirconia specimen and the commonly used Ti implant, and it was

confirmed that there was a significant difference in the degree of cell adhesion and cell proliferation experiments. Similarly, when confirmed through a four-week implantation experiment using rabbits, the HA coating had excellent bone compatibility similar to that of the Ti implant, which was an incomparably increased number compared to the existing zirconia implant.

Collectively, these results suggest that low-temperature sintering sol-gel-derived HA coatings will increase the potential of zirconia in dental applications.

Reference

1. Sykaras N, Iacopino AM, Marker VA, Triplett RG, Woody RDJIIJoO, Implants M. Implant materials, designs, and surface topographies: their effect on osseointegration. A literature review. *The International Journal of Oral & Maxillofacial Implants*. 2000;15(5).
2. Schwitalla A, Müller W-D. PEEK dental implants: a review of the literature. *Journal of Oral Implantology*. 2013;39(6):743-9. doi:10.1563/AAID-JOI-D-11-00002.
3. Mohseni E, Zalnezhad E, Bushroa AR. Comparative investigation on the adhesion of hydroxyapatite coating on Ti-6Al-4V implant: A review paper. *International Journal of Adhesion and Adhesives*. 2014;48:238-57. doi:10.1016/j.ijadhadh.2013.09.030.
4. Le Guehenec L, Soueidan A, Layrolle P, Amouriq Y. Surface treatments of titanium dental implants for rapid osseointegration. *Dental Materials*. 2007;23(7):844-54. doi:10.1016/j.dental.2006.06.025.
5. Kim J, Lee H, Jang T-S, Kim D, Yoon C-B, Han G et al. Characterization of Titanium Surface Modification Strategies for Osseointegration Enhancement. *Metals*. 2021;11(4):618. doi:10.3390/met11040618.

6. Ozkurt Z, Kazazoglu E. Zirconia dental implants: a literature review. *Journal of Oral Implantology*. 2011;37(3):367–76. doi:10.1563/AAID-JOI-D-09-00079.
7. Heydecke G, Kohal R, Gläser R. Optimal esthetics in single-tooth replacement with the Re-Implant system: a case report. *International Journal of Prosthodontics*. 1999;12(2).
8. Cho Y, Hong J, Ryoo H, Kim D, Park J, Han J. Osteogenic responses to zirconia with hydroxyapatite coating by aerosol deposition. *Journal of Dental Research*. 2015;94(3):491–9. doi:10.1177/0022034514566432.
9. Roy M, Bandyopadhyay A, Bose S. Ceramics in Bone Grafts and Coated Implants. *Materials for Bone Disorders*. Elsevier; 2017. p. 265–314.
10. Piconi C, Burger W, Richter H, Cittadini A, Maccauro G, Covacci V et al. Y-TZP ceramics for artificial joint replacements. *Biomaterials*. 1998;19(16):1489–94.
11. Piconi C, Maccauro G. Zirconia as a ceramic biomaterial. *Biomaterials*. 1999;20(1):1–25. doi:10.1016/S0142-9612(98)00010-6.
12. Rahaman MN, Yao A, Bal BS, Garino JP, Ries MD. Ceramics for Prosthetic Hip and Knee Joint Replacement. *Journal of the American Ceramic Society*. 2007;90(7):1965–88. doi:10.1111/j.1551-

2916.2007.01725.x.

13. Zhu Y, Liu K, Deng J, Ye J, Ai F, Ouyang H et al. 3D printed zirconia ceramic hip joint with precise structure and broad-spectrum antibacterial properties. *International Journal of Nanomedicine*. 2019;14:5977–87. doi:10.2147/IJN.S202457.

14. Denry I, Kelly JR. State of the art of zirconia for dental applications. *Dental materials*. 2008;24(3):299–307. doi:10.1016/j.dental.2007.05.007.

15. Osman RB, Swain MV. A critical review of dental implant materials with an emphasis on titanium versus zirconia. *Materials*. 2015;8(3):932–58. doi:10.3390/ma8030932.

16. Ramesh S, Lee KS, Tan C. A review on the hydrothermal ageing behaviour of Y-TZP ceramics. *Ceramics International*. 2018;44(17):20620–34. doi:10.1016/j.ceramint.2018.08.216.

17. Depprich R, Zipprich H, Ommerborn M, Naujoks C, Wiesmann H-P, Kiattavorncharoen S et al. Osseointegration of zirconia implants compared with titanium: an in vivo study. *Head & Face Medicine*. 2008;4(1):30. doi:10.1186/1746-160X-4-30.

18. Gahlert M, Gudehus T, Eichhorn S, Steinhauser E, Kniha H, Erhardt W. Biomechanical and histomorphometric comparison between zirconia implants with varying surface textures and a titanium implant in the maxilla of miniature pigs. *Clinical Oral*

Implants Research. 2007;18(5):662–8. doi:10.1111/j.1600–0501.2007.01401.x.

19. Siddiqui DA, Jacob JJ, Fidai AB, Rodrigues DC. Biological characterization of surface–treated dental implant materials in contact with mammalian host and bacterial cells: titanium versus zirconia. RSC Advances. 2019;9(55):32097–109. doi:10.1039/c9ra06010c.

20. Liu YT, Lee TM, Lui TS. Enhanced osteoblastic cell response on zirconia by bio–inspired surface modification. Colloids and Surfaces B: Biointerfaces. 2013;106:37–45. doi:10.1016/j.colsurfb.2013.01.023.

21. Pajor K, Pajchel L, Kolmas J. Hydroxyapatite and fluorapatite in conservative dentistry and oral implantology—A review. Materials. 2019;12(17):2683. doi:10.3390/ma12172683.

22. Brunton P, Davies R, Burke J, Smith A, Aggeli A, Brookes S et al. Treatment of early caries lesions using biomimetic self–assembling peptides—a clinical safety trial. British dental journal. 2013;215(4):E6–E. doi:10.1038/sj.bdj.2013.741.

23. Suchanek W, Yoshimura M. Processing and properties of hydroxyapatite–based biomaterials for use as hard tissue replacement implants. Journal of Materials Research. 1998;13(1):94–117. doi:10.1557/JMR.1998.0015.

24. Ahn J-H, Kim J, Han G, Kim D, Cheon K-H, Lee H et al. 3D-printed biodegradable composite scaffolds with significantly enhanced mechanical properties via the combination of binder jetting and capillary rise infiltration process. *Additive Manufacturing*. 2021;41:101988. doi:10.1016/j.addma.2021.101988.
25. Awasthi S, Pandey SK, Arunan E, Srivastava C. A review on hydroxyapatite coatings for the biomedical applications: experimental and theoretical perspectives. *Journal of Materials Chemistry B*. 2021;9(2):228-49. doi:10.1039/D0TB02407D.
26. Ong JL, Chan DCN. Hydroxyapatite and Their Use As Coatings in Dental Implants: A Review. *Critical Reviews in Biomedical Engineering*. 2000;28(5-6):667-707. doi:10.1615/CritRevBiomedEng.v28.i56.10.
27. Kong YM, Kim DH, Kim HE, Heo SJ, Koak JY. Hydroxyapatite-based composite for dental implants: an in vivo removal torque experiment. *Journal of Biomedical Materials Research*. 2002;63(6):714-21. doi:10.1002/jbm.10392.
28. Jaafar A, Hecker C, Árki P, Joseph Y. Sol-gel derived hydroxyapatite coatings for titanium implants: A review. *Bioengineering*. 2020;7(4):127. doi:10.3390/bioengineering7040127.
29. Piveteau L-D, Girona M, Schlapbach L, Barboux P, Boilot J-P,

Gasser B. Thin films of calcium phosphate and titanium dioxide by a sol-gel route: a new method for coating medical implants. *Journal of Materials Science: Materials in Medicine*. 1999;10(3):161-7. doi:10.1023/A:1008985423644.

30. Sanosh K, Chu M-C, Balakrishnan A, Kim T, Cho S-J. Sol-gel synthesis of pure nano sized β -tricalcium phosphate crystalline powders. *Current Applied Physics*. 2010;10(1):68-71. doi:10.1016/j.cap.2009.04.014.

31. Kim HW, Kim HE, Salih V, Knowles JC. Dissolution control and cellular responses of calcium phosphate coatings on zirconia porous scaffold. *Journal of Biomedical Materials Research Part A*. 2004;68(3):522-30. doi:10.1002/jbm.a.20094.

32. Deplaine H, Lebourg M, Ripalda P, Vidaurre A, Sanz - Ramos P, Mora G et al. Biomimetic hydroxyapatite coating on pore walls improves osteointegration of poly (L - lactic acid) scaffolds. *Journal of Biomedical Materials Research Part B: Applied Biomaterials*. 2013;101(1):173-86. doi:10.1002/jbm.b.32831.

33. Ishikawa K, Garskaite E, Kareiva A. Sol-gel synthesis of calcium phosphate-based biomaterials—A review of environmentally benign, simple, and effective synthesis routes. *Journal of Sol-Gel Science Technology*. 2020;94(3):551-72. doi:10.1007/s10971-020-05245-8.

34. Oyane A, Kakehata M, Sakamaki I, Pyatenko A, Yashiro H, Ito A et al. Biomimetic apatite coating on yttria-stabilized tetragonal zirconia utilizing femtosecond laser surface processing. *Surface and Coatings Technology*. 2016;296:88–95. doi:10.1016/j.surfcoat.2016.03.075.
35. Quan H, Park YK, Kim SK, Heo SJ, Koak JY, Han JS et al. Surface Characterization and Human Stem Cell Behaviors of Zirconia Implant Disks Biomimetic-Treated in Simulated Body Fluid. *International Journal of Oral & Maxillofacial Implants*. 2016;31(4):928–38. doi:10.11607/jomi.4376.
36. Sharifianjazi F, Pakseresht AH, Asl MS, Esmaeilkhanian A, Jang HW, Shokouhimehr M. Hydroxyapatite consolidated by zirconia: applications for dental implant. *Journal of Composites Compounds*. 2020;2(2):26–34. doi:10.29252/jcc.2.1.4.
37. Hasan MF, Wang J, Berndt C. Evaluation of the mechanical properties of plasma sprayed hydroxyapatite coatings. *Applied surface science*. 2014;303:155–62. doi:10.1016/j.apsusc.2014.02.125.
38. Fawzi M, Madon RH, Sarwani KI, Osman SA, Razali MA, Mohammad AW. Effect of Reaction Temperature on Steam Methane Reforming' s yield over Coated Nickel Aluminide (Ni₃Al) Catalyst in Micro Reactor. *Journal of Advanced Research in Fluid Mechanics*

Thermal Sciences. 2018;50(2):170–7.

39. Gross K, Chai C, Kannangara G, Ben–Nissan B, Hanley L. Thin hydroxyapatite coatings via sol–gel synthesis. *Journal of Materials Science: Materials in Medicine*. 1998;9(12):839–43. doi:10.1023/A:1008948228880.

40. Chung SH, Kim HK, Shon WJ, Park YS. Peri - implant bone formations around (Ti, Zr) O₂ - coated zirconia implants with different surface roughness. *Journal of clinical periodontology*. 2013;40(4):404–11. doi:10.1111/jcpe.12073.

41. Hafezeqoran A, Koodaryan R. Effect of zirconia dental implant surfaces on bone integration: a systematic review and meta–analysis. *BioMed research international*. 2017;2017. doi:10.1155/2017/9246721.

42. Jemat A, Ghazali MJ, Razali M, Otsuka Y. Surface modifications and their effects on titanium dental implants. *BioMed research international*. 2015;2015. doi:10.1155/2015/791725.

43. Shalabi M, Gortemaker A, Hof MVt, Jansen J, Creugers N. Implant surface roughness and bone healing: a systematic review. *Journal of dental research*. 2006;85(6):496–500. doi:10.1177/154405910608500603.

44. Chen S, Guo Y, Liu R, Wu S, Fang J, Huang B et al. Tuning surface properties of bone biomaterials to manipulate osteoblastic

cell adhesion and the signaling pathways for the enhancement of early osseointegration. *Colloids Surfaces B: Biointerfaces*. 2018;164:58–69. doi:10.1016/j.colsurfb.2018.01.022.

45. Gittens RA, Olivares–Navarrete R, Schwartz Z, Boyan BD. Implant osseointegration and the role of microroughness and nanostructures: lessons for spine implants. *Acta biomaterialia*. 2014;10(8):3363–71. doi:10.1016/j.actbio.2014.03.037.

46. Rong M, Lu H, Wan L, Zhang X, Lin X, Li S et al. Comparison of early osseointegration between laser–treated/acid–etched and sandblasted/acid–etched titanium implant surfaces. *Journal of Materials Science: Materials in Medicine*. 2018;29(4):1–6. doi:10.1007/s10856–018–6049–1.

47. Norton J, Malik K, Darr J, Rehman I. Recent developments in processing and surface modification of hydroxyapatite. *Advances in Applied Ceramics*. 2006;105(3):113–39. doi:10.1179/174367606X102278.

48. Jafari MM, Khayati GR. Prediction of hydroxyapatite crystallite size prepared by sol–gel route: gene expression programming approach. *Journal of Sol–Gel Science Technology*. 2018;86(1):112–25. doi:10.1007/s10971–018–4601–6.

49. Yelten A, Yilmaz S. Various parameters affecting the synthesis of the hydroxyapatite powders by the wet chemical precipitation

technique. *Materials Today: Proceedings*. 2016;3(9):2869–76.
doi:10.1016/j.matpr.2016.07.006.

50. Yousefi K, Khalife A. Influence of phosphor precursors on the morphology and purity of sol-gel-derived hydroxyapatite nanoparticles. *Advances in Applied NanoBio-Technologies*. 2021;2(2):49–52.

51. Jin SD, Um SC, Lee JK. Surface Modification of Zirconia Substrate by Calcium Phosphate Particles Using Sol-Gel Method. *Journal of nanoscience nanotechnology*. 2015;15(8):5946–50.
doi:10.1166/jnn.2015.10439.

52. Saiz E, Gremillard L, Menendez G, Miranda P, Gryn K, Tomsia AP. Preparation of porous hydroxyapatite scaffolds. *Materials Science*

Engineering: C

2007;27(3):546–50. doi:10.1016/j.msec.2006.05.038.

53. Kothapalli C, Wei M, Legeros R, Shaw M. Influence of temperature and aging time on HA synthesized by the hydrothermal method. *Journal of Materials Science: Materials in Medicine*. 2005;16(5):441–6. doi:10.1007/s10856-005-6984-5.

54. Rodríguez-Clemente R, López-Macipe A, Gómez-Morales J, Torrent-Burgués J, Castano V. Hydroxyapatite precipitation: a case of nucleation–aggregation–agglomeration–growth mechanism.

- Journal of the European Ceramic Society. 1998;18(9):1351–6.
doi:10.1016/S0955–2219(98)00064–8.
55. Liu D–M, Troczynski T, Tseng WJ. Aging effect on the phase evolution of water–based sol–gel hydroxyapatite. *Biomaterials*. 2002;23(4):1227–36. doi:10.1016/S0142–9612(01)00242–3.
56. Hasegawa A, Kameyama T, Motoe A, UEDA M, AKASHI K, FUKUDA K. Coating of hydroxyapatite on zirconia utilizing a radio–frequency thermal plasma process. *Journal of the Ceramic Society of Japan*. 1992;100(1160):377–81. doi:10.2109/jcersj.100.377.
57. Chiu C–Y, Hsu H–C, Tuan W–H. Effect of zirconia addition on the microstructural evolution of porous hydroxyapatite. *Ceramics International*. 2007;33(5):715–8. doi:10.1016/j.ceramint.2005.12.008.
58. Evis Z. Reactions in hydroxylapatite–zirconia composites. *Ceramics International*. 2007;33(6):987–91. doi:10.1016/j.ceramint.2006.02.012.
59. Kim HW, Kong YM, Koh YH, Kim HE, Kim HM, Ko JS. Pressureless Sintering and Mechanical and Biological Properties of Fluor - hydroxyapatite Composites with Zirconia. *Journal of the American Ceramic Society*. 2003;86(12):2019–26. doi:10.1111/j.1151–2916.2003.tb03602.x.
60. Kim H–W, Noh Y–J, Koh Y–H, Kim H–E, Kim H–M. Effect of

CaF₂ on densification and properties of hydroxyapatite–zirconia composites for biomedical applications. *Biomaterials*. 2002;23(20):4113–21. doi:10.1016/S0142–9612(02)00150–3.

61. Khor K, Fu L, Lim V, Cheang P. The effects of ZrO₂ on the phase compositions of plasma sprayed HA/YSZ composite coatings. *Materials Science and Engineering: A*. 2000;276(1–2):160–6. doi:10.1016/S0921–5093(99)00495–5.

62. Ben Ayed F, Bouaziz J. Sintering of tricalcium phosphate–fluorapatite composites with zirconia. *Journal of the European Ceramic Society*. 2008;28(10):1995–2002. doi:10.1016/j.jeurceramsoc.2008.02.004.

63. Klein C, Driessen A, De Groot K, Van Den Hooff A. Biodegradation behavior of various calcium phosphate materials in bone tissue. *Journal of Biomedical Materials Research*. 1983;17(5):769–84. doi:10.1002/jbm.820170505.

64. Kim H–W, Lee S–Y, Bae C–J, Noh Y–J, Kim H–E, Kim H–M et al. Porous ZrO₂ bone scaffold coated with hydroxyapatite with fluorapatite intermediate layer. *Biomaterials*. 2003;24(19):3277–84. doi:10.1016/s0142–9612(03)00162–5.

65. Kocyło E, Franchin G, Colombo P, Chmielarz A, Potoczek M. Hydroxyapatite–coated ZrO₂ scaffolds with a fluorapatite intermediate layer produced by direct ink writing. *Journal of the*

- European Ceramic Society. 2021;41(1):920–8.
doi:10.1016/j.jeurceramsoc.2020.08.021.
66. Wennerberg A, Albrektsson T. Structural influence from calcium phosphate coatings and its possible effect on enhanced bone integration. *Acta Odontologica Scandinavica*. 2009;67(6):333–40.
doi:10.1080/00016350903188325.
67. Haddow D, James P, Van Noort R. Sol–gel derived calcium phosphate coatings for biomedical applications. *Journal of Sol–Gel Science Technology*. 1998;13(1):261–5.
doi:10.1023/A:1008699421635.
68. Kisi EH, Howard C, editors. Crystal structures of zirconia phases and their inter–relation. *Key Engineering Materials*; 1998: Trans Tech Publ.
69. Feng W, Mu–Sen L, Yu–Peng L, Yong–Xin Q. A simple sol–gel technique for preparing hydroxyapatite nanopowders. *Materials Letters*. 2005;59(8–9):916–9. doi:10.1016/j.matlet.2004.08.041.
70. Kale K, Raskar R, Rane V, Gaikwad A. Carbon Dioxide Adsorption by Calcium Zirconate at Higher Temperature. *Bulletin of Chemical Reaction Engineering Catalysis*. 2012;7(2):124–36.
71. LeGeros RZ. Properties of osteoconductive biomaterials: calcium phosphates. *Clinical Orthopaedics Related Research*. 2002;395:81–98.

72. Chiang Y, Wang C, Akbar S. Calcium zirconate for the monitoring of hydrocarbons. *Sensors and Actuators B: Chemical*. 1998;46(3):208–12. doi:10.1016/S0925-4005(98)00114-2.
73. Lu HB, Campbell CT, Graham DJ, Ratner BD. Surface characterization of hydroxyapatite and related calcium phosphates by XPS and TOF-SIMS. *Analytical chemistry*. 2000;72(13):2886–94. doi:10.1021/ac990812h.
74. Gomes GC, Borghi FF, Ospina RO, López EO, Borges FO, Mello A. Nd:YAG (532 nm) pulsed laser deposition produces crystalline hydroxyapatite thin coatings at room temperature. *Surface and Coatings Technology*. 2017;329:174–83. doi:10.1016/j.surfcoat.2017.09.008.
75. Sakthiabirami K, Vu VT, Kim JW, Kang JH, Jang KJ, Oh GJ et al. Tailoring interfacial interaction through glass fusion in glass/zinc-hydroxyapatite composite coatings on glass-infiltrated zirconia. *Ceramics International*. 2018;44(14):16181–90. doi:10.1016/j.ceramint.2018.05.161.
76. Zhang S, Wang YS, Zeng XT, Khor KA, Weng W, Sun DE. Evaluation of adhesion strength and toughness of fluoridated hydroxyapatite coatings. *Thin Solid Films*. 2008;516(16):5162–7. doi:10.1016/j.tsf.2007.07.063.
77. Revell P, Al-Saffar N, Kobayashi A. Biological reaction to

debris in relation to joint prostheses. Proceedings of the Institution of Mechanical Engineers, Part H: Journal of Engineering in Medicine. 1997;211(2):187–97. doi:10.1243/0954411971534304.

78. Szmukler - Moncler S, Salama H, Reingewirtz Y, Dubruille J. Timing of loading and effect of micromotion on bone–dental implant interface: review of experimental literature. Journal of Biomedical Materials Research. 1998;43(2):192–203. doi:10.1002/(SICI)1097–4636(199822)43:2<192::AID-JBM14>3.0.CO;2–K.

79. Wazen RM, Currey JA, Guo H, Brunski JB, Helms JA, Nanci A. Micromotion–induced strain fields influence early stages of repair at bone–implant interfaces. Acta Biomaterialia. 2013;9(5):6663–74. doi:10.1016/j.actbio.2013.01.014.

80. Zheng X, Huang M, Ding C. Bond strength of plasma–sprayed hydroxyapatite/Ti composite coatings. Biomaterials. 2000;21(8):841–9. doi:10.1016/S0142–9612(99)00255–0.

81. Liu D–M, Yang Q, Troczynski T. Sol–gel hydroxyapatite coatings on stainless steel substrates. Biomaterials. 2002;23(3):691–8. doi:10.1016/S0142–9612(01)00157–0.

82. Weng W, Baptista JL. Preparation and characterization of hydroxyapatite coatings on Ti6Al4V alloy by a sol - gel method. Journal of the American Ceramic Society. 1999;82(1):27–32.

doi:10.1111/j.1151-2916.1999.tb01719.x.

83. Quan R, Zhang L, Xu J, Wang C, Wei X, Yang D. The Bonding Strength of HA/ZrO₂-Layered Biomaterials with Different Interfacial Patterns. *International Journal of Applied Ceramic Technology*. 2015;12(2):273-81. doi:10.1111/ijac.12166.

84. Wei X, Wang C, Li Y, Quan R, Lai Y. Bonding strength of HA/ZrO₂ biomaterials with different interlayers. *Composite Interfaces*. 2016;24(4):357-70.

doi:10.1080/09276440.2016.1210479.

85. Matsumoto TJ, An SH, Ishimoto T, Nakano T, Matsumoto T, Imazato S. Zirconia-hydroxyapatite composite material with micro porous structure. *Dental Materials*. 2011;27(11):e205-12. doi:10.1016/j.dental.2011.07.009.

86. Daisuke Y, Hideo S, Motoharu M, Seiji B. Hydroxyapatite coating on zirconia using glass coating technique. *Journal of the Ceramic Society of Japan* 2008;116(1):20-2. doi:10.2109/jcersj2.116.20.

초 록

치과용 임플란트로서의 지르코니아의 골적합성을 증가시키기 위한 졸 젤 법을 활용한 하이드록시아파타이트 코팅

다양한 이유로 상실되는 치아를 대체하기 위한 치과용 임플란트는 널리 사용되고 있는 경조직 임플란트이다. 치과용 임플란트로 가장 널리 사용되는 재료는 티타늄(Ti)으로 우수한 강도와 생체 친화성을 장점으로 가지고 있다. 하지만 이 티타늄은 금속 특유의 광채를 갖는 표면 때문에 심미적으로 거부감을 갖을 수 있으며, 금속에서의 비특이적 면역 반응과 침 등의 생체 물질에 의한 부식 등이 문제가 되고 있다. 한편 지르코니아는 우수한 기계적 물성과 미적 효과와 부식과 면역 반응에서 자유롭다는 점에서 최근 새로운 치과용 임플란트 소재로 주목 받고 있다. 하지만 지르코니아는 상대적으로 낮은 골적합성을 가지고 있다는 단점이 존재한다. 하이드록시아파타이트는 인체 뼈의 대표적인 구성 물질로 체내에 많이 존재하는 생체 친화성 세라믹이다. 특유의 우수한 생체 친화성 덕분에 수많은 생체 재료의 표면을 코팅하기 위한 재료로 사용되고 있다. 지르코니아의 생체 적합성 향상을 위한 하이드록시아파타이트 (HA) 코팅 관련 연구가 많이 진행되었지만 두꺼운 두께와 고온 소결에서의 부산물 생성 등에 의한 안정성 저하가 문제가 되고 있다.

이 연구에서는 지르코니아의 생체 적합성을 증가시키기 위해 졸-젤법을 이용하여 하이드록시아파타이트를 코팅하고자 한다. 졸-젤법을 이용하여 코팅층의 나노 및 마이크로 구조를 변화시켜 생체 적합성을 더욱 더 증

진시키고, 소결 온도를 조절하여 부산물이 없는 얇고 안정적인 하이드록시아파타이트 코팅 층을 형성하고자 한다.

먼저 하이드록시아파타이트 코팅층의 표면 구조를 변화시키기 위해 소결온도 및 하이드록시아파타이트 졸의 에이징 시간을 조절하였고, 주사전자현미경 (SEM) 관찰을 통해 표면 구조를 관찰하여 소결온도가 나노 구조에, 에이징 시간이 마이크로 구조에 영향을 끼침을 알았다. 또한 투과전자현미경 (TEM) 관찰을 통해 에이징 시간에 따른 하이드록시아파타이트 졸 내의 입자 크기의 변화를 확인하였고, 이 변화가 코팅층의 마이크로 구조 변화의 원인임을 알 수 있었다. 집속 이온 빔 (FIB)을 통한 두께를 측정하였을 때, 코팅 층은 150 nm 정도, 마이크로 구조를 가지는 부분은 800 nm 정도의 크기를 가짐을 확인하였다. 또한 비접촉 3D 표면 분석을 통해 Ra가 마이크로 구조를 가질 경우 350 nm 정도로 마이크로 구조가 없을 때의 100 nm 정도보다 증가함을 확인하였다. 또한 X-선 회절 분석기 (XRD)와 X-선 광전자 분광법 (XPS)을 통해 소결 온도를 섭씨 800도로 진행했을 때 HA와 지르코니아 이외의 결정상은 없던 반면, 1000도로 진행했을 때 불순물인 칼슘 지르코네이트가 생성된 것을 확인하였다. 코팅층과 지르코니아의 접착 강도는 Instron을 통한 tensile test로 진행되었고, 약 40 MPa 이상의 값을 가져 치과용 임플란트 응용 분야로 적절하였다.

이런 부분들을 종합하여 섭씨 800도 조건 하에 마이크로 구조의 형성을 조절하여 조골 세포를 통한 세포 실험을 진행하였고, 마이크로 구조를 가지는 경우가 세포 특성이 증가함을 확인하였다. 이를 바탕으로 생체

내 동물 실험을 비교군인 티타늄과 더불어 하이드록시 아파타이트가 코팅된 지르코니아와 지르코니아에 실행한 결과, 지르코니아의 골 적합성이 하이드록시 아파타이트 코팅에 의해 극적으로 향상됨을 입증했으며, 이는 기존 티타늄 임플란트와 비슷한 수준이었다.

이 연구를 통해 하이드록시 아파타이트를 통한 지르코니아의 골적합성 증가를 이뤄낼 수 있었다. 또한 하이드록시아파타이트 졸의 에이징 시간 및 소결 시간을 조절하여 코팅 층의 나노 및 마이크로 구조를 조절할 수 있었으며, 특히 소결 시간을 조절하여 지르코니아와 하이드록시아파타이트의 부산물인 칼슘 지르코네이트의 생성을 억제할 수 있었다. 이를 기반으로 생성한 졸 젤 기반 HA 코팅 지르코니아가 치과용 임플란트 재료로 사용하기에 큰 잠재력을 가지고 있음을 세포 실험 및 생체 내 동물 실험을 통해 입증하였다.

주요어: 치과용 임플란트, 지르코니아, 하이드록시아파타이트, 표면 개질, 졸-젤, 골융합성

감사의 글 (Acknowledgement)

뜻뜻한 마음을 가지고 처음으로 관악을 밟았던 날이 벌써 햇수로 12년이 되었습니다. 설렘을 가득 안고 이십대를 시작하던 어린이가 이제 삼십대가 되어 사회의 구성원이 되기 위해 관악을 떠나게 됩니다. 그 기간 동안 마음으로는 많이 변하지 않았다고 생각하지만 외적으로나 내적으로 많은 변화를 겪었겠죠. 그런 변화들이 지금의 저를 만들었다고 생각합니다. 그리고 그런 변화들은 학부와 대학원 생활을 지내며 만난 수많은 사람들에게 많은 배움과 도움 없이는 이루질 못 했을 것입니다. 그 모든 분들에게 감사의 마음을 담아 짧게나마 표현해보고자 합니다.

가장 먼저 물리적으로나 정신적으로나 지금의 저를 만들어주신 부모님에게 감사의 말씀을 드려야겠습니다. 언제나 저의 첫번째는 부모님이시고 가족입니다. 항상 사랑하고 걱정하고 생각하고 있지만 그런 부분들을 많이 표현해드리지 못한 부분들이 죄송스러워 마음 한 켠에 남아 있습니다. 계속해서 공부를 하고 싶은 제 욕심에 이제 편하게 쉬실 연세이신 부모님에게 아직 많은 부분을 기대고 있는 부분 또한 죄송합니다. 앞으로는 편하게 쉬실 수 있도록 더 많이 효도하도록 할게요.

비록 육체적으로 나이를 먹어 장성한 아들이지만 아직 사회적으로는 어리기만 한 막내 아들을 매일매일 걱정하시는 아버지에게 감사드립니다. 저에게 직접적으로 표현하시진 않으시지만 누구보다도 저의 선택을 존중해주시고 믿어주시고 지원해주셔서 감사합니다. 아직 미답기만 한 막내이지만 앞으로 믿음직스러운 아들이 될 수 있도록 노력할게요. 사랑합니

다. 그리고 올해 환갑을 맞이한 엄마에게 저는 언제나 걱정스럽기만 한 아들입니다. 저는 아직 부족한 부분이 많아 무슨 일이 있을 때마다 엄마를 찾는 철부지이지만 앞으로는 스스로 더 많은 부분을 해내어 걱정하지 않는 아들이 되도록 하겠습니다. 그리고 앞으로는 더 자주 찾아 뵈어 지금까지 받은 것 이상으로 줄 수 있는 아들이 되겠습니다. 그렇게 자주 전화하면서도 사랑한다는 말을 하지 못 하는데 이 자리를 빌어 사랑한다는 말을 전하고 싶습니다.

그리고 타지에서 생활하고 있어 만나지 못 하는 우리 형에게도 감사의 말을 전합니다. 비록 물리적 거리가 멀어 자주 연락하지는 못 하지만 형이 해주는 조언 한 마디, 그리고 심리적으로 기댈 수 있다는 형제가 있다는 사실 자체가 나에게 큰 보물과도 같다고 생각해. 형은 어렸을 때부터 지금까지 나의 자랑이야. 그래서 언제나 나에게 옳은 사람이었고, 내 삶의 이정표와 같아. 앞으로도 쪽 어리기만 한 동생이겠지만, 나도 형에게 기댈 수 있는 사람이 되도록 할게. 형이 원하는 모든 일이 잘 이루어지길 바라고 사랑해.

제가 박사학위를 받을 수 있게끔 지원해주신 김현이 교수님에게 감사의 말씀을 드립니다. 부족한 저를 지도해주주시고 훌륭한 연구를 하실 수 있게 지원해주셔서 아직도 부족하지만 박사 학위를 가진 연구자로 만들어 주셔서 감사합니다. 교수님께서 지도해 주셨던 부분들, 그 모든 조언들이 저의 연구 생활의 지침이 되었습니다. 그 지침들을 앞으로의 연구 생활에서도 소중하게 생각하며 지키도록 하겠습니다. 교수님의 제자로 남을 수 있다는 사실에 감사드리며 앞으로 연구자의 길을 걸으면서 교수

님의 명성에 누가 되지 않도록 노력하겠습니다. 언제나 인자한 웃음으로
맞이해주시던 교수님의 모습을 잊지 못 할 것입니다. 항상 건강하시고
행복하시길 바랍니다.

그리고 귀한 시간을 내주셔서 저의 박사 학위 과정을 심사해주신 안철
희 교수님, 선정운 교수님, 한철민 교수님, 정현도 교수님에게 감사드립니다.
교수님들의 조언 덕분에 연구의 부족한 부분을 알 수 있었고 한층
더 발전시킬 수 있는 기회를 얻었습니다. 교수님들이 해주신 조언들을
명심하겠습니다.

한철민 교수님과 정현도 교수님에게는 다시 한 번 감사의 말씀을 드립니다.
저의 연구 과정을 지도해주셨고, 여러 논문을 작성하는데 도움을
주셔서 저의 연구를 진행하도록 많은 도움을 주셨습니다. 교수님들과 함
께 연구를 진행했던 경험이 저의 소중한 밑거름이 될 것입니다.

이외에도 대학원을 다니는 동안 수많은 사람들을 만나서 박사학위를 무
사히 끝낼 수 있었습니다. 그 중에서 가장 먼저 감사의 인사를 전해야하
는 사람은 대략 6년의 시간 동안 기숙사에서 나와 함께 생활하였던 영
환이입니다. 대학원 생활 동안 함께 생활하는 룸메였고, 가장 오래 만났
던 취향이 맞는 친구이며, 함께 생활한 가족이었어. 우리가 그 긴 시간
동안 정말 많은 취미들을 함께 했고, 정말 많은 이야기를 나눴다. 서로
볼꼴 못 볼꼴도 많이 봤고. 돌이켜보면 내가 좋은 룸메였는지는 잘 모르
겠어. 하지만 나에게 영환이가 최고의 룸메였어. 내가 대학원 생활을 즐
겁게 보낼 수 있었던 일등공신은 너였다고 생각한다. 그래서 한없이 고
마워. 앞으로 우리가 지금까지처럼 자주 만나긴 힘들겠지만 그래도 지금

처럼 서로 힘든 일, 좋은 일을 나눌 수 있는 친구이자, 형제처럼 지낼 수 있길 바래. 앞으로 좋은 일이 가득하길!

BMA 연구실을 다니면 만났던 모든 분들에게도 감사합니다. 가장 먼저 연구실을 든든하게 지켜주고 많은 것을 알려주신 이성미 박사님에게 감사의 말씀을 드립니다. 그리고 처음 들어와서 아무것도 모르던 신입생이던 저를 이끌어주시던 선배님들, 성원이 형과 새미 누나, 재욱이 형, 호용이 형, 병석이 형, 설하 누나, 민호 형에게 먼저 감사의 말을 전합니다. 그리고 얘기를 많이 나누진 못 했지만 항상 즐거운 에너지를 주던 chen ke에게도 감사의 말을 전합니다. 직접적으로 교류를 많이 하던 선배들 중에서 저의 버팀목이 되어줬던 현이 형! 형이 해줬던 이야기들을 잊지 못 할 거 같아요. 앞으로도 연구를 진행하면서 서로 도울 수 있으면 좋겠어요. 그리고 한참 위에 있는 하늘 같은 선배이지만 같은 나이여서 기댈 수 있었던 광희. 연구분야는 많이 달랐지만 너의 경험을 듣는 것만으로 큰 도움을 받았어. 그리고 시간을 아끼지 않고 모든 걸 알려주던 천일이. 같은 나이이기도 해서 귀찮게 한 일이 많은데 한번도 귀찮아하지 않고 친절히 알려줘서 고마워. 그리고 처음에 도움을 많이 줬던 이제 아기가 아빠가 된 은호. 배울 점이 많았는데 빠르게 졸업해서 많이 못 배운 게 아쉽네. 같은 야구 팬이고 모두에게 웃음을 자주 주던 경일. 너의 그 유머 감각은 잊지 못할 것 같아. 그리고 가장 많은 시간을 보낸 선배 중 한 명이었던 인구. 내가 퍽퍽대고 살갑게 대하지 않아도 다가와주고 많은 이야기를 나눌 수 있는 사람이 되어줘서 고맙다. 그리고 동기 석우. 처음에 많이 힘들어할 때 더 큰 도움을 주지 못 한 부분이 아직 마음에

남아 있고, 그럼에도 불구하고 좋은 동기가 되어줘서 고맙다. 그리고 끝까지 함께 한 민규. 항상 긍정적인 에너지를 가지고 있고, 힘든 일을 함께하는 동기가 되어줘서 고마워. 마지막까지 함께하는 유이한 후배 창하와 수형이. 정말 많은 걸 함께 했고 내가 엄청 부족한 선배임에도 잘 따라주고 친하게 지내준 점이 고맙다. 창하에게는 와인을 알려준 선생님의 생각하고 연구실에서 가장 친한 친구로 남아줘서 고마워. 수형이에게는 항상 귀찮게 했던 거 같은데 그래도 성격 좋게 받아줘서 고맙다. 그리고 마지막으로 수영을 하며 더 친해진 다영 누나와 윤정이. 수영을 배운 건 건강해진 것도 있지만 두 사람과 친해질 수 있는 기회를 얻어서 내가 대학원 다니면서 가장 잘 한 일 중 하나라고 생각해. 내가 본 사람 중에 가장 활동적인 다영 누나. 누나의 그 활발한 에너지 덕분에 많은 사람을 만날 수 있었고, 많은 활동을 할 수 있었어. 그리고 취향 맞는 친구였던 윤정이. 술도 좋아하고 얘기하는 것도 좋아해서 내가 얘기하는 정말 쓸데 없는 시시콜콜한 얘기들을 잘 들어줘서 고마워. 하고 싶은 말은 많지만 간단하게 한 줄씩 적었습니다. 이렇게 적다 보니 대학원에서 만난 모든 사람들이 다들 좋은 사람이었다는 생각이 듭니다. 모든 사람들에게 고맙고, 그 모든 사람들에게 나도 좋은 사람이었길 바랍니다. 그리고 앞으로도 모든 사람들에게 좋은 사람이 될 수 있도록 노력할게요. 다들 건강하고 행복하고 바라는게 이루어지길 진심으로 바랍니다.

그리고 가장 좋은 친구로 남아주었던 우리 재료과 10학번 동기들, 그리고 야구동아리 플레이보이즈 선배, 후배 여러분에게도 감사의 말씀을 드립니다. 감사드릴 사람들이 너무나 많아 일일이 모든 사람들에게 감사

의 말을 전할 순 없겠지만 이런 친구들이 근처에 있다는 것만으로 제가 얼마나 운이 좋은 사람인지 알 수 있었습니다. 힘든 일이나 기쁜 일이 있을 때 만나서 감정을 나눌 수 있는 사람들이어서 대학원 생활을 더 활기차게 보낼 수 있었습니다. 감사의 마음을 담아 모든 사람들의 행복을 기원할게요.

마지막으로 기다긴 대학원 생활 동안 버팀목이 되어준 사랑하는 연주에게 감사의 말을 남깁니다. 연주가 없었다면 대학원 생활이 잿빛이었을텐데 연주 덕분에 유채색의 생활을 하게 해줘서 고마워.

적은 사람들 이외에도 저의 대학원 생활을 응원해주신 많은 사람들 그리고 지탱해주신 많은 사람들, 친척 분들과 친구 분들 모두에게도 감사의 말을 드립니다. 감사드릴 사람이 이렇게나 많다는 것은 저의 행복이라고 생각해요. 이 모든 분들에게 저도 하나의 행복이 될 수 있도록 살아가고 싶습니다. 모든 사람들의 행복을 기원하며 이만 감사의 글을 줄이도록 하겠습니다.